 Bull. Chem. Soc. Jpn., 74, 889—906 (2001)

Synthesis and Properties of Head-to-head, Head-to-tail, and Tail-to-tail Orientational Isomers of Extended Dihexylbithiophene–Octaethylporphyrin System [OEP–(DHBT)$_n$–OEP] Connected with 1,3-Butadiyne Linkages

Hiroyuki Higuchi,* Takashi Ishikura, Kazumine Mori, Yukari Takayama, Koji Yamamoto, Keita Tani,† Keiko Miyabayashi,†† and Mikio Miyake††

Department of Chemistry, Faculty of Science, Toyama University, 3190 Gofuku, Toyama, Toyama 930-8555

†Division of Natural Science, Osaka Kyoiku University, 4-698-1 Asahi-oka, Kashiwara, Osaka 582-0026

††School of Materials Science, JAIST (Hokuriku), 1-1 Asahi-dai, Tatsunokuchi, Noumi, Ishikawa 923-1292

(Received September 18, 2000)

An extended π-electronic conjugation system of dihexylbithiophene–octaethylporphyrin [OEP–(DHBT)$_n$–OEP; n = 1–5], all the chromophores in which are connected with the linkage of 1,3-butadiyne (diacetylene), was synthesized by an oxidative cross-coupling reaction of the corresponding terminal acetylenes. Absorption spectral and electrochemical properties of the OEP–(DHBT)$_n$–OEP system were examined. The results proved that the orientation of two 3-hexylthiophene (3HTh) rings of DHBT plays an important role in electronic communications between the two terminal OEP rings.

In recent years, a wide variety of the thiophene (Th) derivatives have been synthesized, because of their high susceptibilities to the light and electronic stimulations, in order to develop new functional organic materials such as opto-electronic devices.[1] Previously, we studied the syntheses and structural properties of the oligo(3-hexylthiophene) derivatives from the viewpoint of the π-electronic conjugation planarity,[2] and suggested that the orientation of two 3-hexylthiophene (3HTh) rings in the dihexylbithiophene (DHBT) constituent plays an important role in their electronic and electrochemical behaviors.[3] In particular, from the studies of the donor–acceptor DHBT derivatives was proved experimentally a structure–property relationship of the higher third-order nonlinear optical (NLO) behaviors with the more extended π-electronic conjugation systems.[4]

On the other hand, particularly in the last decade, the researches on the porphyrin-based oligomers and arrays have been vastly extended,[5] for the sake of molecular architectures such as molecular switch, light-harvest, and energy- and electron-transfer systems. We have been also engaged in the studies on the structural and electronic properties of the large-membered heterocyclic compounds such as aza-annulene[6] and octaethylporphyrin (OEP) nuclei,[7] in which the linkage of 1,3-butadiyne (diacetylene) is incorporated in the conjugation chain as a useful tool for making the π-electronic conjugation system more rigid and extended.

Since the diacetylene linkage was preliminarily found to participate in the π-electronic conjugation with the DHBT chromophore efficiently,[8] a hybridized system between DHBT and OEP chromophores connected with the diacetylene linkage (OEP–DHBT–OEP; **1**,[9] **2**, and **3**[9]) (Chart 1) has been designed and synthesized. In this system, the two 3HTh rings of DHBT are linked with head-to-head (HH), head-to-tail (HT), and tail-to-tail (TT) orientations. In the course of the synthesis of **1** and **3**, the more extended conjugation systems describable as OEP–(DHBT)$_n$–OEP (n = 2–5; **17** for **1** and **18** for **3**) (Chart 4) were simultaneously obtained.

Our continuous interests are basically to examine whether or not DHBT works well as a controlling unit for the electronic communications between two terminal function sites and then to derive the structural requirements for an enhancement of the particular electronic properties from the comparative studies. Here, we wish to report the syntheses of the title compounds **1**–**3**, **17**, and **18** and of the related conjugation system 3HTh–OEP (**4** and **5**) (Chart 2), and also wish to discuss their structural properties, as compared with electronic and electrochemical features from the viewpoint of the π-electronic conjugation planarity.

Results and Discussion

Synthesis. According to our conventional method for preparation of the diacetylene-group connected derivatives,[6–9] the title OEP–DHBT–OEP system was constructed by the oxidative cross-coupling reaction of the *meso*-ethynyl substituted OEP **9**[10] with the corresponding α,ω-diethylnyl substituted DHBT (**8**, **12**, or **15**), as shown in Scheme 1.

The compounds **8**, **12**, and **15** were prepared from the corresponding orientational dibromo-DHBT **6**,[3a] **10**,[3a] and **13**[3a] with trimethylsilylacetylene {[HC≡CSi(CH$_3$)$_3$]; TMSA}, under the Sonogashira conditions,[11] followed by alkaline hydrolysis. In

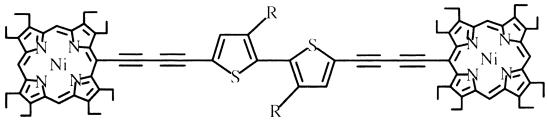

$R=C_6H_{13}$

1

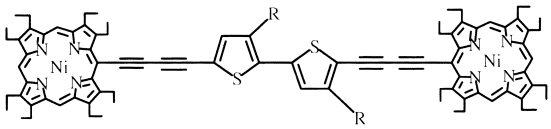

2

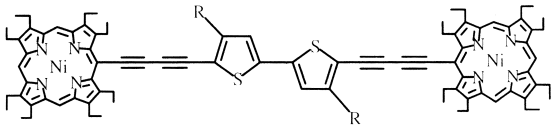

3

Chart 1.

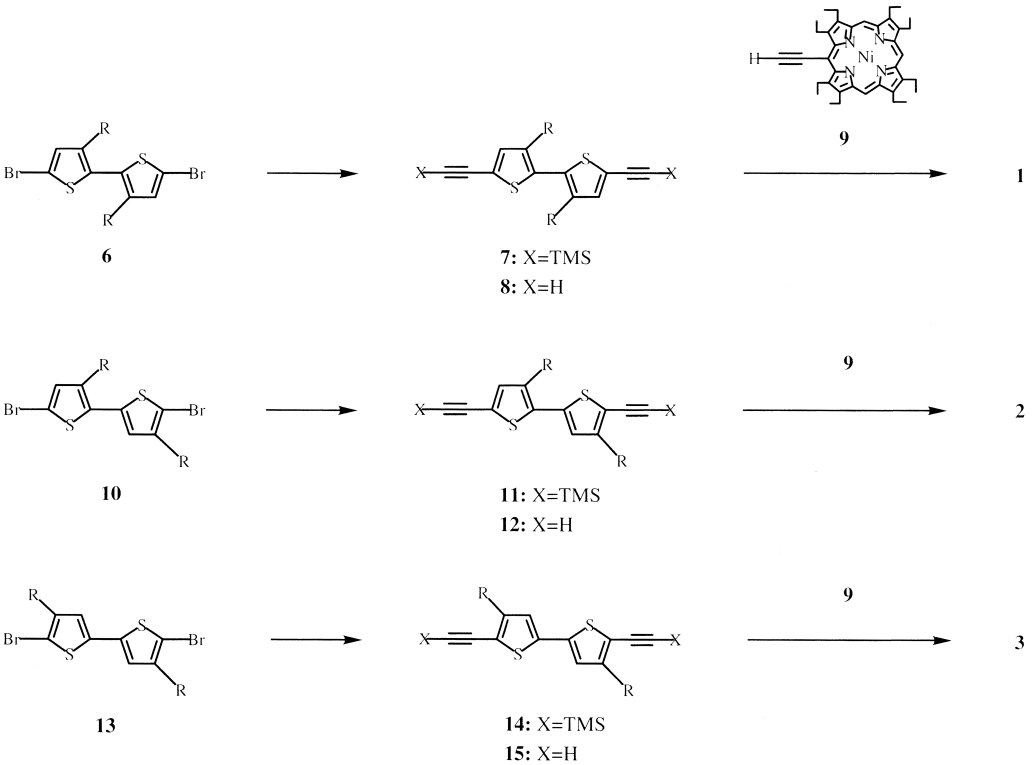

Scheme 1.

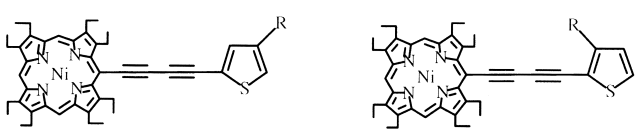

4 **5**

Chart 2.

the case of the symmetrical compounds **1** and **3** of the OEP–DHBT–OEP system, coupling reactions of **8** and **15** with 2.2 molar amounts of **9** were carried out in the presence of anhydrous copper(II) acetate [$Cu(OAc)_2$] in a mixture of pyridine and methanol (Py:MeOH = 5:1); modified Eglinton conditions.[12] Yields of **1** and **3** were optimized to reach up to 15% and 20% yields based on **8** and **15**,[9] together with 31% and 21% yields of the diacetylene-group connected OEP dimer **16**[10] from the respective reactions (Chart 3). Under these con-

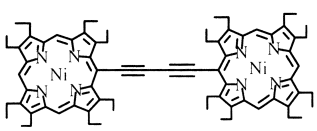

16

Chart 3.

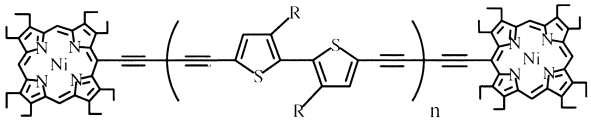

17: n=2-5

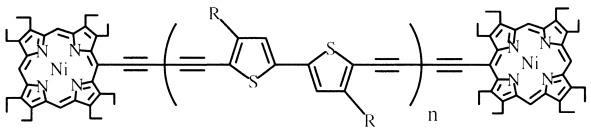

18: n=2-5

Chart 4.

ditions, the compounds of type **17** described as OEP–(DHBT)$_n$–OEP, which contain two, three, four, and five units of the α,ω-diethynyl substituted DHBT component (n) between the two terminal OEP rings of the HH isomer **1**, were simultaneously obtained in 13%, 10%, 7%, and 4% yields based on **8**, respectively (Chart 4). All the compounds were successfully separated by repeated column chromatography on silica gel, which were eluted in order of molecular weight from the compound with $n = 5$ to the compound with $n = 0$ (**16**). This was also the case for the TT isomer **3**, similarly affording the compounds of type **18** in 16% ($n = 2$), 26% ($n = 3$), 8% ($n = 4$), and 11% ($n = 5$) yields based on **15**, respectively. From the fact that the stoichiometry between the terminal acetylenes of DHBT and OEP for the present cross-coupling reaction can be regarded as almost equivalent in one reaction site, while the DHBT constituent is distributed much more in the products of types **17** and **18** than **1** and **3**, one may conclude that the terminal acetylene of DHBT is more reactive than that of OEP under the Eglinton conditions. This would be supported by evidence that a greater amount of the OEP reactant **9** suppresses the formation of the products like **17** and **18** with the greater n (also see vide infra). The structures of **1** and **3** as well as the by-products **17** and **18** could be easily and definitely determined by MS and ^{1}H NMR spectral measurements (vide infra).

In contrast with C_2 symmetrical OEP–(DHBT)$_n$–OEP system of types **17** and **18**, the corresponding by-products from the reaction for the HT isomer **2** would be expected to result in a fairly complicated situation. Although the compound **2** corresponding to $n = 1$ possesses only one structure, the possible orientational isomers as the by-products increase in number tremendously with an increase of n, due to the loss of symmetry of the DHBT moiety. For example, in the case of $n = 2$, it is easily expected that three compounds exist as the possible isomers, as shown in Chart 5. However, in the case of $n = 5$, sixteen compounds should exist as the possible isomers, suggesting that separation of the reaction mixture into each product will be difficult. Therefore, we decided to achieve the synthesis of **2** under the conditions which suppress the formation of the by-products as much as possible by using an excessive amount of the *meso*-ethylnyl OEP **9** to the diethynyl HT DHBT **12**. After several examinations, when the cross-coupling reaction of **12** with 3.8 molar amounts of **9** was carried out under high dilution conditions, the desired compound **2** was obtained in a fair yield of 26%, togheher with 36% yield of **16**. In this reaction, few by-products with more than $n = 3$ were formed, as expected. Although the by-product with $n = 2$ (ca. 5% yield) was ascertained and proved to be composed of more than two isomers on the bases of ^{1}H NMR and MS spectral measurements (see Experimental), the separation of this isomeric mixture to each product was abandoned due to the high similarity in all physical properties.

Along with compounds of **1**–**3**, the diacetylene-group connected 3HTh–OEP derivatives **4** and **5** were synthesized in a similar way, as shown in Scheme 2. The 5-ethynylthiophene derivative **21** as a counterpart for **4** was prepared by starting from the selective ethynylation of 2,5-dibromo-3-hexylthiophene (**19**),[2] since the 5-position in the parent 3HTh is less reactive to the ordinary electrophilic substitutions than the counter-side 2-position.[13] Ethynylation of **19** with an equimolar amount of TMSA occurred at 5-position preferably, due to less steric hindrance, to afford the 5-ethynylthiophene derivative **20** (ca. 60%) which was readily submitted to alkaline hydrolysis to give **21** in a quantitative yield. On the other hand, the 2-ethynylthiophene derivative **24** was prepared from 3-hexyl-2-iodothiophene (**22**),[14] since the ethynylation of the corresponding 2-bromothiophene derivative with TMSA exhibited poor yield and reproducibility. Thus, reaction of **22** with TMSA afforded **23** (90%), which was hydrolyzed with an alkaline reagent to give 2-ethynyl-3-hexylthiophene (**24**) quantitatively. Then, cross-coupling reactions of **9** with large molar amounts of the 2- and 5-ethynylthiophene **21** and **24** under the

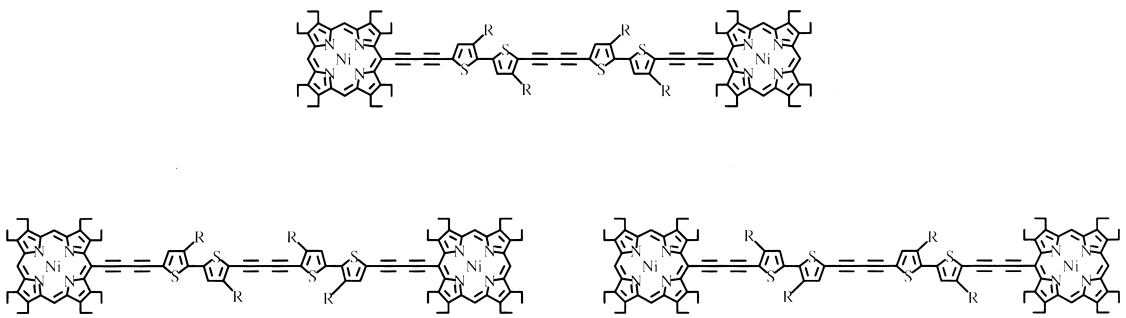

Chart 5.

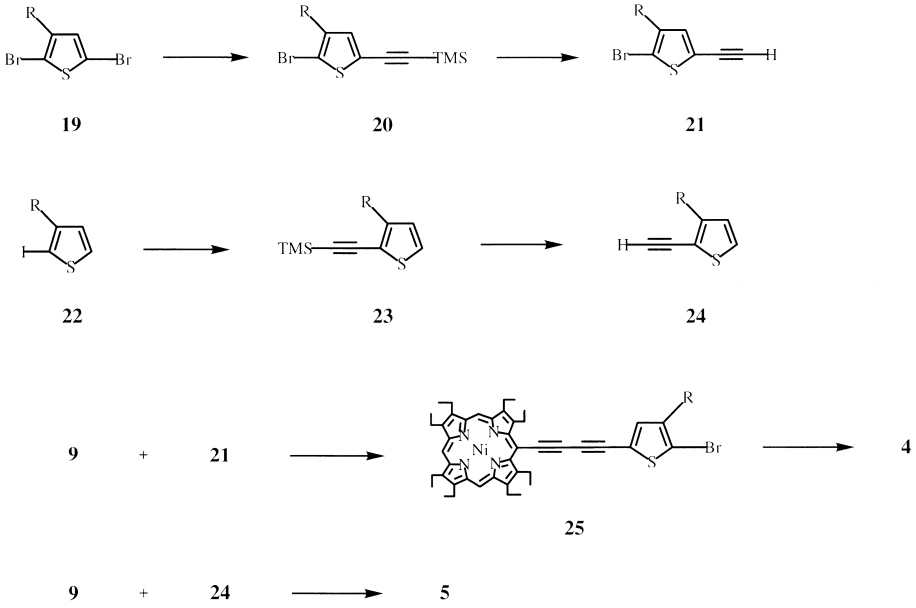

Scheme 2.

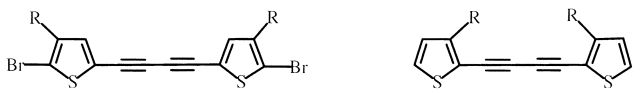

26 27

Chart 6.

modified Eglinton conditions afforded the corresponding diacetylene-group connected compounds **25** and **5** in 57% and 41% yields, respectively. In these reactions, the diacetylene-group connected Th dimers **26** and **27** were simultaneously obtained as the side products in quantity (Chart 6), but little dimeric OEP **16** was formed. Then, the former compound **25** was treated with lithium aluminum hydride (lithium tetrahydridoaluminate: $LiAlH_4$) to give the compound **4** quantitatively.

Mass Spectra. Mass spectral measurements of the OEP–DHBT–OEP system **1–3** were attempted by FAB technical method. This FAB technical method, however, was found to be ineffective for most of the compounds in the more extended OEP–$(DHBT)_n$–OEP system **17** and **18**, as was the EI technical method, probably due to both their high molecular weights and hard ionizations. Thus, the structures of **17** and **18** were primarily ascertained by ESI-FT-ICR technical method,[15] which has been recently developed. The present method is very effective for detection not only of the ordinary species but also of particular species such as macromolecular ions, short-life ions with a few fragments, and multi-charged ions. In the case of type **17**, for example, the compound with $n = 5$ was observed degrading in fairly simple fragments (Fig. 1). Although no mono-charged ion peak at around m/z 3130 was given, the spectrum clearly showed fragmentation patterns at

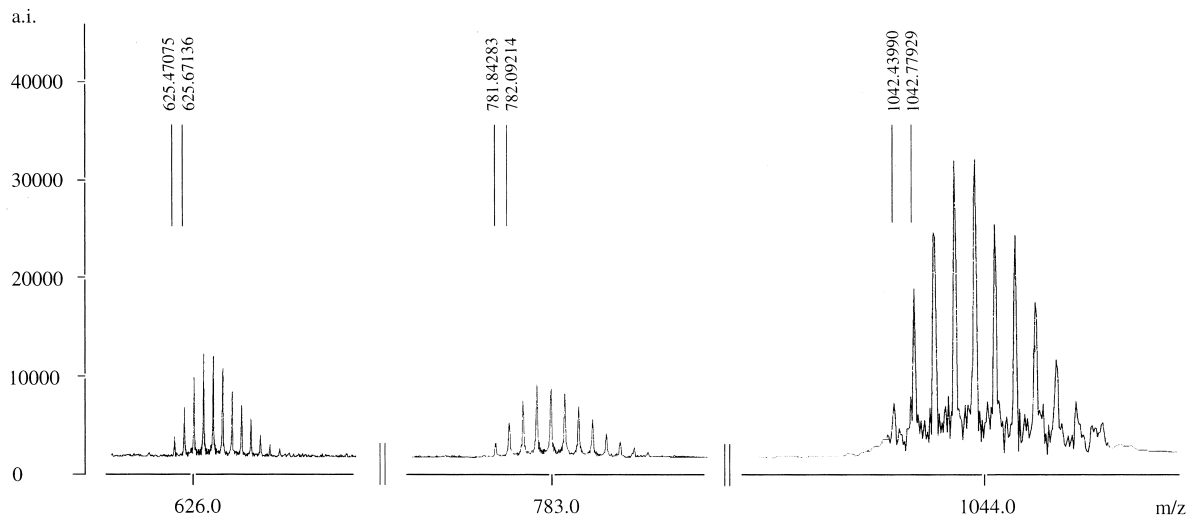

Fig. 1. Mass scale-expanded view of signals near m/z 626, 783, and 1044 for HH isomer (**1**).

Table 1. Chemical Shifts of the Selected Protons for the OEP–DHBT–OEP and 3HTh–OEP Systems and the Related Compounds in $CDCl_3$ and THF-d_8 at 25 °C

Compounds[a)]	$CDCl_3$		THF-d_8	
	meso-H	Th–H	*meso*-H	Th–H
1	9.42 (4H)	7.33 (2H)	9.51 (4H)	7.47 (2H)
	9.40 (2H)		9.49 (2H)	
2	9.42 (4H)	7.24 (1H)	9.50 (4H)	7.39 (1H)
	9.39 (2H)	6.99 (1H)	9.48 (2H)	7.16 (1H)
3	9.42 (4H)	7.00 (2H)	9.51 (4H)	7.25 (2H)
	9.39 (2H)		9.48 (2H)	
4	9.41 (2H)	7.25 (1H)	9.49 (2H)	7.34 (1H)
	9.39 (1H)	6.95 (1H)	9.47 (1H)	7.14 (1H)
Ni–OEP	9.76 (4H)		9.84 (4H)	
3HTh		7.23 (1H)		7.25 (1H)
		6.93 (1H)		6.96 (1H)
		6.91 (1H)		6.91 (1H)

a) **1**–**3**: 1.0–1.1 × 10^{-3} mol cm^{-3}. **4**, Ni–OEP, and 3HTh: 2.0–2.3 × 10^{-3} mol cm^{-3}.

around *m*/*z* 1044 (0.33930 Da) which correspond to triply-charged ion peaks, patterns at around *m*/*z* 783 (0.24931 Da) which correspond to quadruply-charged ion peaks, and patterns at around *m*/*z* 626 (0.20061 Da) which correspond to quintuply-charged ion peaks. Similarly, the main molecular ion peaks (M^+) for the other compounds of type **17** were observed as *m*/2*z* 933.93665 for $n = 2$, *m*/2*z* 1183.99047 for $n = 3$, and *m*/3*z* 916.08107 for $n = 4$. The fact that the fragmentations of **17** by means of ESI-FT-ICR technical method are prone to generate multi-charged ions would not be due to the structural properties of the OEP–DHBT–OEP system but rather due to the Ni complex of the materials, as is generally known.[15] No particular difference in fragmentations was observed between HH and TT orientational isomers, and thus, the results of **18** were very similar to those of **17** (see Experimental).

^{1}H NMR Spectra. ^{1}H NMR spectral measurements of the OEP–DHBT–OEP and 3HTh–OEP systems were performed in $CDCl_3$ at room temperature, unless otherwise stated. Chemical shifts of the selected protons of the compounds are given in Table 1. All the spectra of the OEP–DHBT–OEP system are fairly simple, reflecting their high symmetrical structures, as shown in the spectrum for the TT isomer **3** (Fig. 2). Nevertheless, in the case of **2** with HT orientation of DHBT, the 3HTh ring protons (Th–H) appeared separately at 7.24 ppm and 6.99 ppm, respectively, due to its unsymmetry element, among which the former Th–H exhibited a chemical shift closer to that of the HH isomer **1** ($\delta = 7.33$) and the latter one a chemical shift closer to that of the TT isomer **3** ($\delta = 7.00$). This result indicates that the diacetylene linkage affects the nearer Th–H more intensively through its anisotropic effect,[6] causing a lower field shift of Th–H for **1** than for **3**. Similarly, with respect to the methylene protons belonging to the ethyl substituents at 3,7-positions of OEP and belonging to the hexyl substituents of DHBT, the unsymmetrical structural property of **2** caused a different signal appearance from those of **1** and **3**, affording the unresolved multiplet lines for **2** in contrast with the first-order triplet lines for both **1** and **3**. On the other hand, the

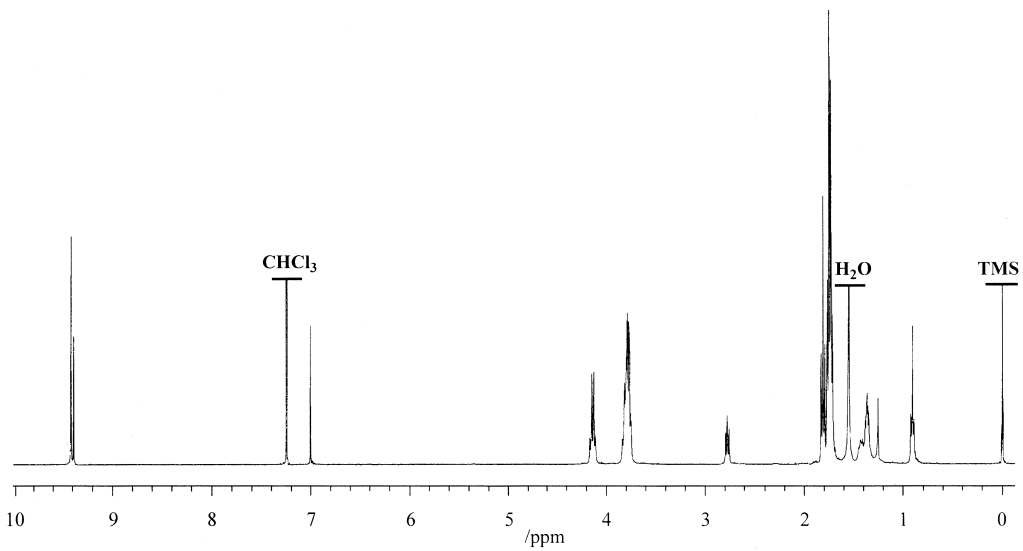

Fig. 2. ^{1}H NMR spectrum of TT isomer (**3**) of the OEP–DHBT–OEP system (400 MHz, $CDCl_3$, 25 °C).

respective OEP *meso*-protons (*meso*-H) exhibited almost the same chemical shifts for these three isomers, appearing at 9.42 (4H) and 9.39 ppm (2H) as the singlet lines, respectively. In consequence, it can be concluded that all the hybrids **1**–**3** substantially possess almost the same structures in bond distances and geometries from the magnetic viewpoint because of their rigid and straight skeletons, though just a little difference in chemical shifts due to the anisotropic effect from the diacetylene linkage was observed between them.

As mentioned above, one of the two Th–H of **2** appeared at 7.24 ppm in $CDCl_3$ solution, due to which the signal was completely buried under the signal of the undeuterated chloroform ($CHCl_3$). Due not only to this eventuality in chemical shift but also to the two signals from *meso*-H found by means of 400 MHz NMR, the structural assignment of **2** was uncertain until a satisfactory result from MS spectral measurements was obtained. Accordingly, when preliminarily measured in perdeuteriotetrahydrofuran (THF-d_8) in place of $CDCl_3$, the spectrum of **2** afforded a helpful result in confirmation of the structure assignment. Chemical shifts due to *meso*-H and Th–H of **2** in THF-d_8 were also summarized in Table 1, as well as those of the isomers **1** and **3** and the related compounds **4**, OEP, and 3HTh. Although the signals due to *meso*-H of **2** still appeared as two singlet lines, the referred Th–H resonated at a fairly low field region of 7.39 ppm in THF-d_8. In this respect, it is worthy of note that not only this Th–H but also another Th–H of **2** shifted to the low fields as much as ca. 0.15 ppm in THF-d_8. Also, the *meso*-H of **2** themselves exhibited the low field shifts in THF-d_8 by ca. 0.1 ppm from the corresponding ones in $CDCl_3$. Furthermore, it was proved that all the protons of ethyl and hexyl substituents of **2** shifted slightly to the low field regions as well, as compared with those in $CDCl_3$ (see Experimental).

The above-mentioned solvent effect on chemical shifts may include a finding for self-association of the OEP–DHBT–OEP system, based on the following reasons. Unlike Th nuclei, porphyrin nuclei including OEP are well known to associate with each other at the higher concentrations due to van der Waals interaction between them.[16] In such a highly concentrated solution as for ^{1}H NMR spectral measurement, for example, the self-association of OEP would cause the high field shift of *meso*-H due to an anisotropic effect from its large diamagnetic ring current,[17] as compared with the less associated OEP solutions. In view of this characteristic behavior of porphyrin derivatives, Table 1 seems to derive the fact that the OEP–DHBT–OEP system **1**–**3** also associates with each other. It shows that *meso*-H of OEP itself resonated at the field higher by 0.08 ppm in $CDCl_3$ (δ = 9.76) than those in THF-d_8 (δ = 9.84), indicating that self-association of OEP heightens in $CDCl_3$ and lowers in THF-d_8. The fact that THF lowers self-association of OEP would probably arise from its strong coordination power as an axial ligand with the central Ni(II) ion of OEP, rather than from its poor solvation power for stabilization of the OEP assembly.[18] On the other hand, Th–H of 3HTh in $CDCl_3$ resonated at almost the same fields as those in THF-d_8, indicating that 3HTh itself is not affected by these solvents in terms of self-association at all. In contrast with these facts for OEP and 3HTh, the OEP–DHBT–OEP system **1**–**3** exhibited some peculiar behaviors. As described above, the corresponding *meso*-H showed the same chemical shifts between **1**–**3**, and yet all the *meso*-H exhibited the high field shifts by almost the same magnitudes of ca. 0.1 ppm by changing THF-d_8 to $CDCl_3$, similarly to those of OEP. On the other hand, the Th–H of **1**–**3** exhibited the outstandingly high field shifts in $CDCl_3$, for example, by 0.14 ppm for **1** and 0.25 ppm for **3**; such values are distinct from those of 3HTh itself. A similar trend in chemical shift changes was also observed for the 3HTh–OEP system **4**, in which not only did *meso*-H shift to the high field by 0.08 ppm but also the referent Th–H shifted by ca. 0.1 ppm in $CDCl_3$. Furthermore, all the ethyl and hexyl protons of **1**–**3** and **4** were found to shift slightly to the high field regions in $CDCl_3$. Since all the *meso*-H of **1**–**3** and **4** exhibited the same behaviors as those of OEP at all points, these results suggest that self-associations of both OEP–DHBT–OEP and 3HTh–OEP systems take place at the sites of OEP constituents and yet more efficiently in $CDCl_3$ than in THF-d_8, reflecting their orientations of DHBT in some ways.[19]

The more extended OEP–$(DHBT)_n$–OEP system of types **17** and **18** is of interest as the molecular wires in terms of such rigid and long skeletons.[1,5] From the molecular model examinations, the compound with n = 5 can be estimated to be 80 Å in length between two center-to-center OEP rings, as shown in Chart 7. Here, it is curious to see the chemical shift behaviors due to Th–H in these compounds. Obviously, on going from n = 1 to n = 5, Th–H named H_a, H_b, H_c, H_d, and H_e in order from the OEP site adds newly to the previous compound by ones with increases of n, resulting in the same number kinds of Th–H as n. The signal changes of Th–H for the compounds of type **17** with HH orientation in THF-d_8, for example, are shown in Fig. 3. Although *meso*-H scarcely changes in chemical shift in all the compounds of type **17**, Th–H separates into the respective regions. All H_a resonate at around 7.45 ppm and all H_b at around 7.38 ppm, while all the other H_c, H_d, and H_e resonate at nearly the same region of 7.36 ppm. This reseult indicates that the anisotropic effect from 18π-electron ring current of OEP induces Th–H to shift to the lower field, suggesting that all the Th–H including those for n = 1 (**1**–**3**) exist within a deshielded region of the OEP ring.[17] However, it is also clearly indicated that an anisotropic effect from the OEP nickel complex (Ni–OEP) along a rod direction of the OEP–$(DHBT)_n$–OEP system no longer affects the third Th–H (H_c) which is estimated to be apart by ca. 25 Å from the nearer OEP, as illustrated in Fig. 4. Anderson also reported an excellent study on the ring current effect of Zn–OEP of the closely-related dimeric OEP and successfully predicted chemical shifts with good accuracy using Abraham's 16 dipole model,[20] in which the two Zn–OEP rings are fixed with the diacetylene linkage with a center-to-center distance of ca. 13 Å.[21] The chemical shifts of Th–H, however, should be influenced by many factors apart from OEP ring current. In this respect, it is also curious to examine the areas influenced from the metallated OEP with different ring currents in the present rigid skeletal system, for example, using a series of Ni–, Pd–, and Pt–OEP complexes of **17** and **18**,[22] synthesis of which is now under way. The above-mentioned tendency in chemical shifts was similarly observed for the compounds of type **18** with TT orientation (see Experimental). Their chemical shift differences between H_a–H_e, however, were much smaller than the corre-

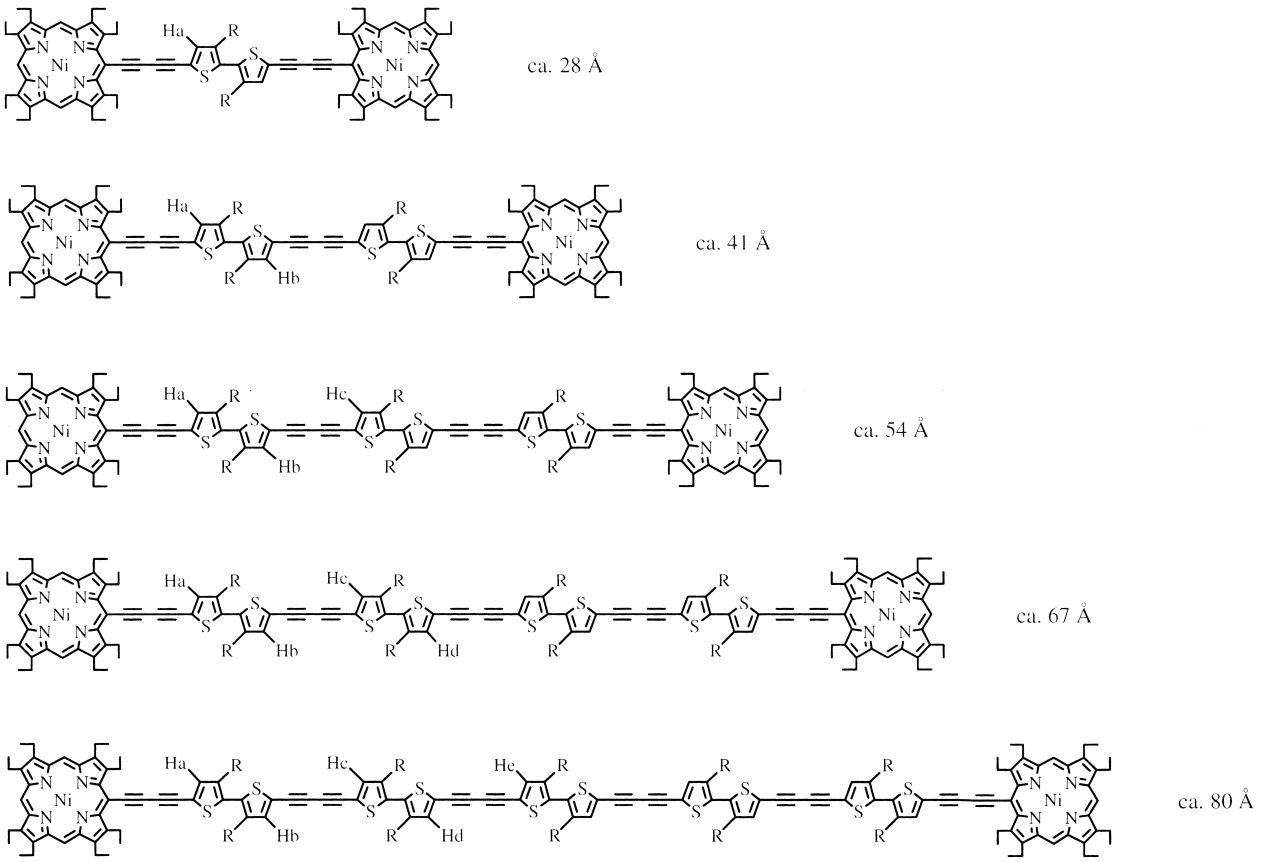

Chart 7.

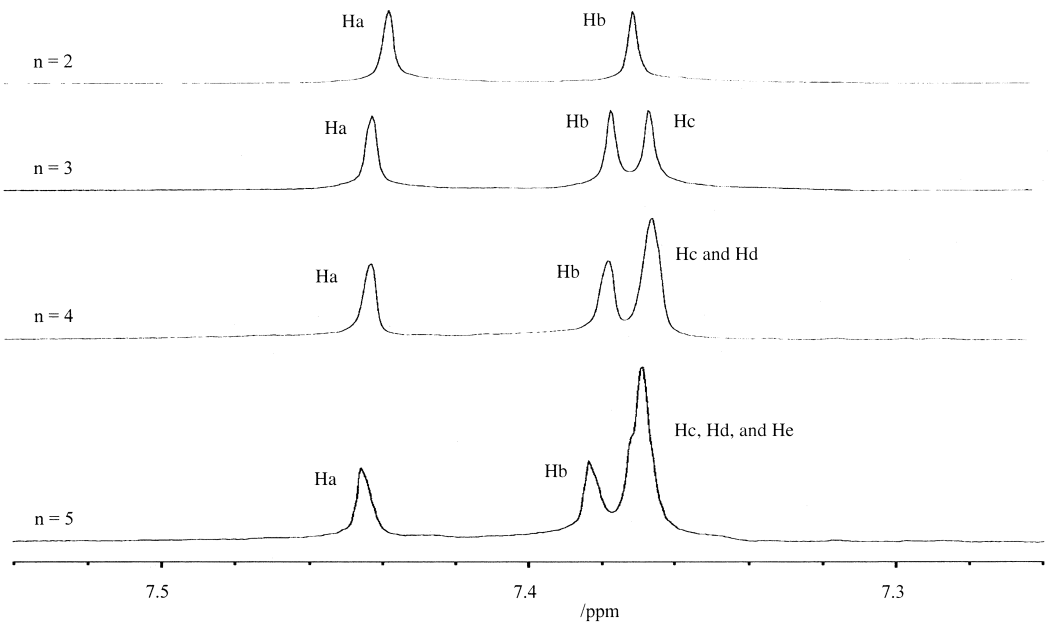

Fig. 3. Th–H signal changes for the OEP–$(DHBT)_n$–OEP system of type **17** (400 MHz, THF-d_8, 25 °C).

sponding ones of type **17**, because all the Th–H of type **18** are almost free from an anisotropic effect of the diacetylene linkage.

Electronic Absorption Spectra. Electronic absorption spectral measurements of the OEP–DHBT–OEP system **1–3** were performed in $CHCl_3$ at room temperature, using almost the same concentrated solutions equivalent in one Ni–OEP nucleus. Their spectral data as well as those of the related com-

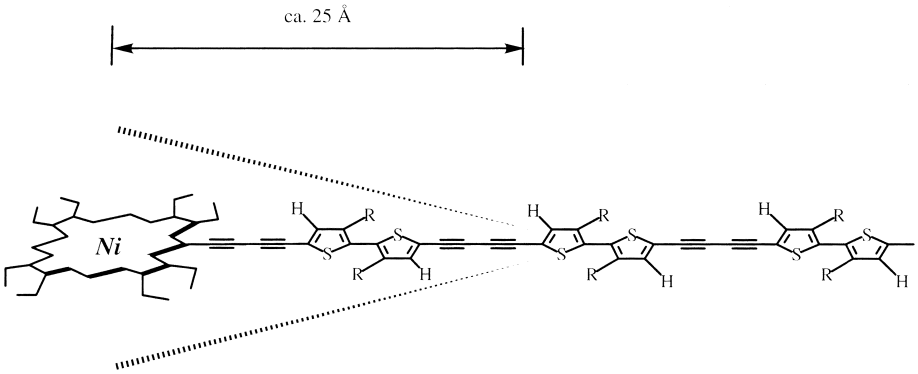

Fig. 4. Boundary distance of the region deshielded by an anisotropic effect due to the Ni–OEP ring current in the OEP–(DHBT)$_n$–OEP system.

Table 2. Maxima (nm) and Intensities (ε) of Soret and Q Bands of OEP–DHBT–OEP, 3HTh–OEP, and the Related Derivatives Connected with the Diacetylene Linkages ($CHCl_3$, 25 °C)

Compounds[a)]	Soret bands			Q bands	
1	435 (178000, sh)	454 (190000)		562 (24500, sh)	593 (28000)
2	440 (146500)	471 (133000)		564 (26000, sh)	599 (43500)
3	440 (134000)	484 (143000)		565 (29000, sh)	601 (52000)
4	445 (144900)			573 (12200)	602 (12300)
5	442 (149200)			574 (12000)	603 (12500)
16	427 (112800)	457 (114400)	484 (130600)	566 (35000, sh)	593 (57300)
28	428 (182000)			556 (7000)	598 (10000)

a) **1**–**3** and **16**: 1.1–1.3 $\times$ 10^{-5} mol cm^{-3}. **4**, **5**, and **28**: 2.1–2.5 $\times$ 10^{-5} mol cm^{-3}.

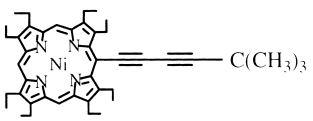

28

Chart 8.

pounds are summarized in Table 2. It is known that Ni–OEP affords the well-characterized absorption bands in $CHCl_3$ at 370 nm (ε 27500, sh) and 393 nm (ε 234400) for Soret band and at 516 nm (ε 11500) and 552 nm (ε 37000) for Q band.[23] As shown in Table 2, an introduction of the diacetylene linkage into Ni–OEP at the *meso*-position (**28**) (Chart 8) induces the considerable changes in both absorption maxima and curves,[24] indicating that an electronic reconstruction takes place between Ni–OEP and diacetylene linkage efficiently to form an extended π-electronic conjugation system. However, it is interesting to note that **28** affords a quite simple spectrum, in spite of the loss of a high molecular D_{4h} symmetry element of Ni–OEP. Furthermore, the combination of 3HTh with **28** (**4** and **5**) did not affect the electronic structure of **28** so intensively as to change its absorption curve, only shifting the respective bands to the longer wavelength regions more or less. This result suggests that 3HTh in this system behaves itself like an electron-donating substituent,[2] similar to the *t*-butyl group, simply causing an elevation of HOMO level of **28**. It is also obvious that the substitution position of the hexyl group in the system of **4** and **5** has no influence on their electronic properties at all. In contrast with the spectral behaviors of **4**, **5**, and **28**, the diacetylene-group connected Ni–OEP dimer **16** exhibits a spectrum characteristic of the strong interaction between the two Ni–OEP rings through the diacetylene linkage, in which the Soret band splits into three bands at maxima of 427, 457, and 484 nm and the Q band increases its molecular extinction co-efficient intensively.[25] It is curious that an introduction of the (*E*)-vinylene linkage in place of the diacetylene linkage between two Ni–OEP rings of **16** scarcely affects the Soret band, with respect to the spectrum of Ni–OEP, but rather affects the Q band intensively, to afford some very characteristic weak bands up to 800 nm.[22]

Various DHBT derivatives show some curious properties reflecting an orientation of the DHBT moiety, which are sometimes hard to predict just from the properties of 3HTh itself.[3,4,8] Similarly, **1**–**3** showed the peculiar feature in their electronic structures, reflecting the respective orientations of DHBT.[9] As shown in Fig. 5, the spectrum (a) for the HH isomer **1** exhibited mainly two separated bands characteristic of the Ni–OEP chromophore, affording the slightly broad Soret band at around 450 nm and the Q band at around 600 nm. On the other hand, the spectra (b) and (c) for the HT and TT isomers **2** and **3** exhibited mainly three bands, in consequence of Soret band splitting into two bands named λ_1 and λ_2 provisionally. Between the two separated bands of Soret band for **2** and **3**, the shorter wavelength absorption bands (λ_1) both exhibited the maxima at 440 nm with reducing the intensity from that for **1**, while the longer wavelength absorption bands (λ_2) exhibited the different maxima at 471 nm for **2** and 484 nm for **3**. In this respect, the maximum λ_2 for **1** might be described as nearly the

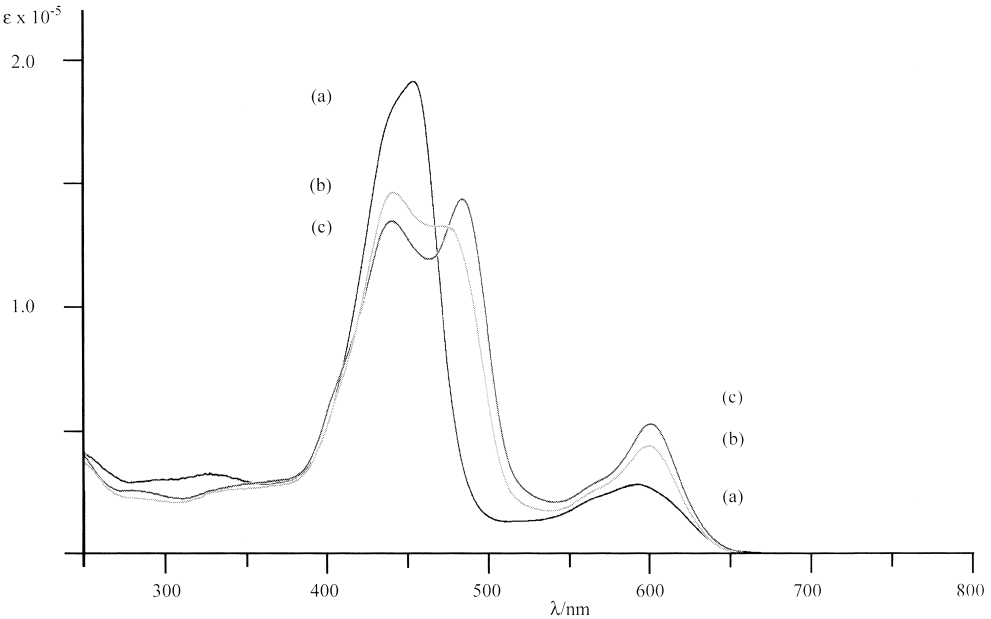

Fig. 5. Electronic absorption spectra of the OEP–DHBT–OEP system ($CHCl_3$, 25 °C): (a) for HH isomer (**1**), (b) for HT isomer (**2**), and (c) for TT isomer (**3**).

same value as that of λ_1, since a different absorption band can be observed as a shoulder at 435 nm. The intensity ratios of these split Soret bands were reversed between **2** and **3**, in which the shorter λ_1 band is less intensive (the longer λ_2 band is more intensive) for the TT isomer **3**. Moreover, the intensities of Q bands increased in order of **1** < **2** < **3**. These results suggest that the electronic interaction between the two Ni–OEP rings takes place through both the diacetylene linkage and the DHBT moiety, with reflection of the extension magnitudes in the π-electronic conjugation depending on the respective orientations of DHBT,[26] to form a new extended π-electronic system. In other words, the electronic interactions between the two Ni–OEP rings, probably via exciton coupling mechanism,[22,25,27] strengthen in the same order of **1** ≪ **2** < **3** as that of the molecular planarities for π-electronic conjugation, also causing an enhancement of their transition probabilities for Q bands in the same order.

As compared with the spectral behaviors of the related compounds, it might be concluded that HH isomer **1** possesses the very similar electronic structure to **4** (or **5**), comparable to a dimeric character of **4** (or **5**). In this case, the HH DHBT itself can not participate efficiently in the π-electronic conjugation with Ni–OEP through the diacetylene linkage, because the two 3HTh rings are twisted about the pinch bond so much as to interrupt the conjugation due to the steric hindrance between the hexyl group and the sulfur atom belonging to the opposite Th ring.[26] On the other hand, the electronic structures of the HT and TT isomers **2** and **3** are rather comparable to that of **16**, in which the central DHBT components participate in the π-electronic conjugation throughout the whole molecule due to their highly planar conformations.[4,8] Such characteristic features of DHBT, where HH isomer behaves itself as a dimeric character of 3HTh, while both HT and TT isomers exist in the extended system hybridized between two 3HTh rings,[2,3] also appear in the electronic properties of the OEP–DHBT–OEP system. These findings indicate that DHBT would play an important role in the electronic communication and transmittance between two terminal chromophores as the functional sites,[1,5] where all the wide-ranging efficiencies of the particular electronic properties can be performed at the molecular level by controlling the conformational planarity, for example, by choosing the orientations of DHBT and/or by introducing any other alkyl substituents including the hexyl group on DHBT.[28]

In the case of the more extended OEP–$(DHBT)_n$–OEP system, on going from $n = 1$ (**1**) to $n = 5$, spectra of the HH orientational series **17** became much broader at around 400 nm and their absorption maxima shifted slightly to the shorter wavelengths (Fig. 6a). On the other hand, the TT isomeric series **18** exhibited a different behavior from **17**, in which the two λ_1 and λ_2 maxima of Soret band at 440 and 484 nm for the compound with $n = 1$ (**3**) tend to gather stepwise and to fuse into the longer wavelength λ_2 band at around 480 nm, with increases of n (Fig. 6b). These results could also be ascribed to differences of the conformational planarities between the HH and TT DHBT constituents. As a result, the electronic structures of the HH series gradually separate into two main characteristic features with increases of n; one arises from the diacetylene-group connected 3HTh–OEP component like **4** (or **5**) and another arises from the remaining $(HH\ DHBT)_n$ component, affording their combined broad spectra, as illustrated in Fig. 7a. On the other hand, the TT series extends its electronic conjugation system between Ni–OEP and DHBT through the diacetylene linkages with increases of n, which may result in some reduction of the HOMO-LUMO energy differences. However, an extension of the π-electronic conjugation of this type simultaneously would weaken the electronic interaction between the terminal Ni–OEP rings, because the two terminal Ni–OEP rings move in the opposite direction and exist apart from each other by ca. 13 Å for every one increment of n (Chart 7). It is likely that such an extension of the π-electronic

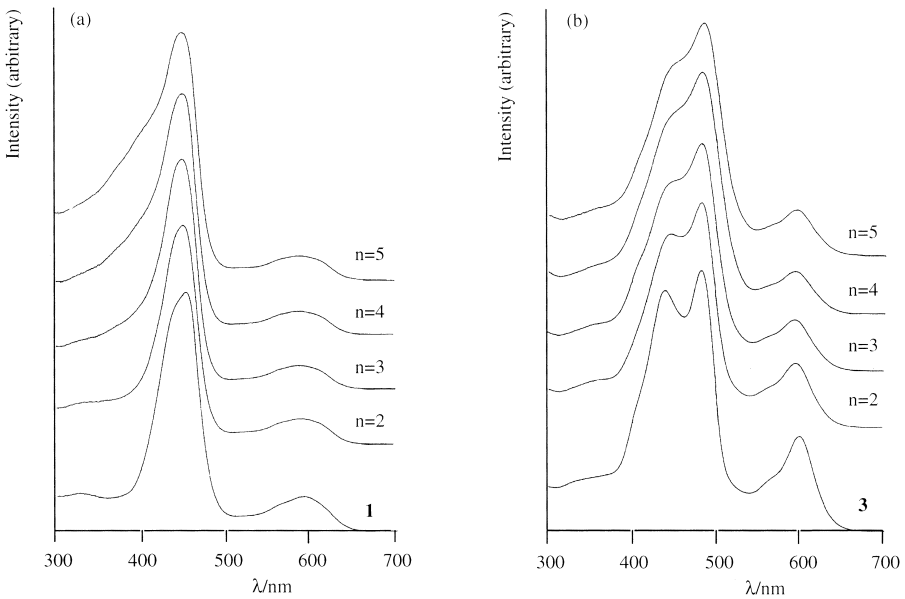

Fig. 6. Electronic absorption spectral changes of the OEP–$(DHBT)_n$–OEP system of types **17** (a) and **18** (b) ($CHCl_3$, 25 °C).

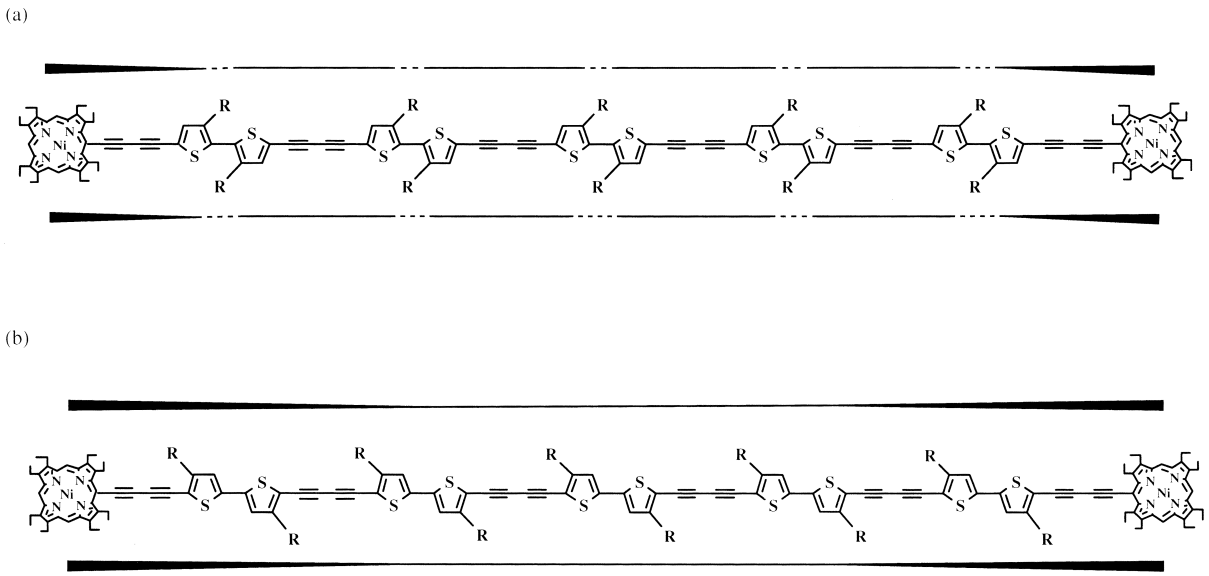

Fig. 7. Characteristic features of the extended π-electronic conjugation system for OEP–$(DHBT)_5$–OEP. (a) for HH isomer and (b) for TT isomer.

conjugation induces a gradual recovery of the structurally unsymmetrical but electronically degenerated structures for the TT series as well. Thus, it is tentatively proposed at present that the TT series converges with increases of n into the hybridized electronic structure between the diacetylene-group connected OEP–(TT DHBT) component and the remaining $(TT\ DHBT)_n$ component (Fig. 7b).[29]

Cyclic Voltammetry. Oxidation potentials of the OEP–DHBT–OEP system **1–3** as well as the related compounds were measured by cyclic voltammetry in dichloromethane (CH_2Cl_2) at room temperature, using sample solutions with almost the same concentrations equivalent in one Ni–OEP nucleus. Their half-wave oxidation potentials ($E^{1/2}$) are summarized in Table 3 and the voltammograms of **1–3** are given in Fig. 8. The numbers of the transferred electrons were analyzed by the respective peak current ratios and the electron-releasing abilities were estimated from the first oxidation potential values ($E_1^{1/2}$). All of these OEP derivatives were oxidized stepwise in a region between −0.2 V and +1.8 V vs SCE, similarly to the other mono- and dinucleic Ni–OEP derivatives,[7,22] indicating that the diacetylene linkage is not critically affected by the electrochemical stimulation within the present potential region. As is seen from Table 3, the oxidations of the compounds **1–3** and **16** bearing two OEP nuclei could be analyzed to proceed via three one-, one-, and two-electron transfer processes. Similarly, the compounds **4** and **5** were also oxidized

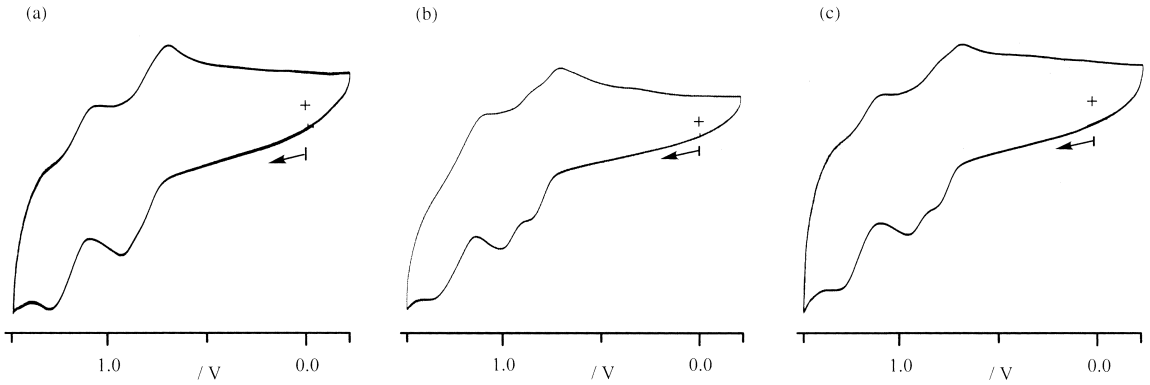

Fig. 8. Cyclic voltammograms of the OEP–DHBT–OEP system (CH_2Cl_2, 25 °C): (a) for HH isomer (**1**), (b) for HT isomer (**2**), and (c) for TT isomer (**3**).

Table 3. Half-Wave Oxidation Potentials (/V)[a)] of OEP–DHBT–OEP and the Related Derivatives Connected with the Diacetylene Linkages

Compounds[b)]	$E_1^{1/2}$	$E_2^{1/2}$	$E_3^{1/2}$
1	0.88 (1e)	0.96 (1e)	1.33 (2e)
2	0.84 (1e)	1.01 (1e)	1.36 (2e)
3	0.82 (1e)	0.96 (1e)	1.29 (2e)
4	0.90 (1e)	1.26 (1e)	
5	0.90 (1e)	1.27 (1e)	
16	0.86 (1e)	1.01 (1e)	1.35 (2e)

a) Oxidation potentials were measured at 25 °C in CH_2Cl_2 containing *n*-Bu_4NClO_4. GC (working *E*), Pt (counter *E*), and SCE (reference *E*). Scan rate; 120 mV s^{-1}. b) 1.2–1.4 $\times$ 10^{-3} mol cm^{-3} for **1–3** and **16** and 2.3–2.6 $\times$ 10^{-3} mol cm^{-3} for **4** and **5**.

stepwise via two one-electron transfer processes. Based on the fact that the oxidation of Ni–OEP proceeds via two one-electron transfer processes under the same conditions to afford the corresponding dicationic species for the final product ($E_1^{1/2}$ = 0.86 V and $E_2^{1/2}$ = 1.32 V),[22,30] the final products from **1–3** and **16** were tentatively assigned to be the corresponding bis(dicationic) species, as illustrated in Scheme 3, and the final products from **4** and **5** were taken to be the mono(dicationic) species as well.

Table 3 also shows that the first oxidation products, which should be assigned to be the radical cations, form more readily from the dinucleic derivatives (**1–3** and **16**) than from the mononucleic ones (**4** and **5**). The radical cations from **1–3** formed at the respective $E_1^{1/2}$ values in order of **1** > **2** > **3**, indicating the lowest electron-releasing ability of **1** ($E_1^{1/2}$ = 0.88 V) and the highest ability of **3** ($E_1^{1/2}$ = 0.82 V). This result indicates that the TT isomer **3** possesses the highest HOMO level in this group and thus exists in the most planar conformation for the π-electronic conjugation throughout the molecule of this extended system at the neutral state, as deduced from the absorption spectral studies. The electron-releasing abilities of **1–3** are correlated not only with the maxima behaviors of their Q bands, as is generally the case,[30] but also with the behavior of λ_2 maxima of Soret bands; the higher ability for the compound with the longer wavelength λ_2 band. The diacetylene-group connected OEP dimer **16** exhibited an inbetween elec-

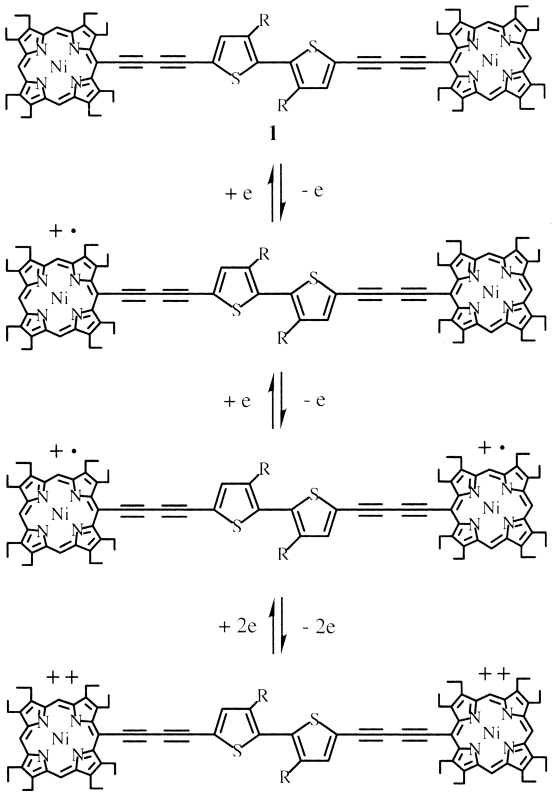

Scheme 3.

tron-releasing ability ($E_1^{1/2}$ = 0.86 V), suggesting that the extension magnitude of the π-electronic conjugation system for **16** is greater than that for the HH isomer **1** but smaller than that for the TT isomer **3**. In other words, the electron-releasing ability of **16** is almost comparable to that of the HT isomer **2**, in terms of an electronic effect arising from the extension magnitude of the conjugation system. These facts also support the conclusion that the HH isomer **1** possesses the dimeric character of **4**. And yet, the substitution position of the hexyl group in the 3HTh–OEP system of **4** and **5** has no influence on the electrochemical properties at all, in accordance with the high similarity in their electronic absorption spectral behaviors. In this respect, the hexyl substituent can be regarded simply as a group controlling the conformational planarities of DHBT, di-

rectly related to the respective steric hindrances arising from the different substitution positions. Additionally, in connection with the electronic and electrochemical behaviors of **16**, it is notable that the diacetylene linkage hardly affects the HOMO level of Ni–OEP, while the (*E*)-vinylene linkage raises the HOMO level of Ni–OEP ($E_1^{1/2} = 0.62$ V) efficiently.[22]

The products from the dinucleic OEP derivatives formed at the second oxidation stage could be the mono(dication)s or the bis(radical cation)s. However, taking the electrostatic repulsion into consideration, the bis(radical cation)s would be more stable than the mono(dication)s in the rigid skeletal system, though an elucidation of the interactive features between the two radical cation sites should wait for further studies of their conformational properties. Therefore, the final products, bis(dicationic) species, are proposed to form directly from the corresponding bis(radical cation)s via a two-electron transfer process, as shown in Scheme 3. The differences ($\Delta E_{2-1}^{1/2}$) between oxidation potential values of $E_1^{1/2}$ and $E_2^{1/2}$ are smaller for the HH isomer **1** ($\Delta E_{2-1}^{1/2} = 0.08$ V) than for the other dinucleic OEP derivatives ($\Delta E_{2-1}^{1/2}$ = ca. 0.15 V), as also seen from the almost overlapped waves between the first and second oxidation stages for **1** (Fig. 8a). On the other hand, the differences ($\Delta E_{3-2}^{1/2}$) between oxidation potential values of $E_2^{1/2}$ and $E_3^{1/2}$ are ca. 0.35 V for all the dinucleic OEP derivatives. These results clearly indicate that the difference in orientations of DHBT affects the stabilization of the mono(radical cation)s more intensively than the bis(radical cation)s, since the on-site Coulomb repulsions between the two radical cation sites can be estimated to be the same in **1**–**3** because of the same distance between them.[2,3a] As derived from the absorption spectral studies, it can be also concluded that the orientation control of DHBT serves as a simple but useful tool for construction of the multi-step electron transfer systems.

In the case of the OEP–$(DHBT)_n$–OEP system, the first oxidation waves for the HH series **17** were found to shift toward the second wave observed for **1** with increases of *n*, resulting in almost a two-step oxidation reaction to the final bis(dicationic) species for the compound with $n = 5$ ($E_1^{1/2} = 0.92$ and $E_2^{1/2} = 1.36$ V). On the other hand, the TT isomeric series **18** proceeded clearly via three steps of electron transfer process to the final oxidation products, similar to **3**, but heightened their $E_1^{1/2}$ values little by little with increases of *n* ($E_1^{1/2} = 0.87$, $E_2^{1/2} = 0.97$, $E_3^{1/2} = 1.38$ V for the compound with $n = 5$). These results would indicate that the electron-releasing abilities of the HH orientational series **17** are determined essentially by a particular structural component in the molecule, i.e., the diacetylene-group connected 3HTh–OEP like **4**, since the respective oxidized products are expected to be hardly stabilized by the resonance effect through the π-electronic conjugation due to the low molecular planarities, similarly to those from **1**. This is closely related with a finding from the absorption spectral studies that the HH series of the OEP–$(DHBT)_n$–OEP system **17** are transformed into the electronic structure regardable as a dimeric character of **4** with increases of *n*. On the other hand, the TT orientational series **18** lower their HOMO levels regularly with increases of *n*, in accordance with the hypsochromic shift of Q band maxima in the same order (Fig. 6b and see Experimental). Also, this result may provide an experimental evidence that the electronic structure of **18** converges into a hybridized feature between the diacetylene-group connected OEP–(TT DHBT) component and the remaining (TT $DHBT)_n$ component with increases of *n* (Fig. 7b).[29]

Conclusion

The extended hybridized OEP–DHBT–OEP system **1**–**3** has been successfully synthesized by oxidative cross-coupling reactions of the corresponding terminal acetylenes under the modified Eglinton conditions. Under the same reaction conditions as for the symmetrical isomers of **1** and **3**, the more extended system **17** and **18** describable as OEP–$(DHBT)_n$–OEP ($n = 2$–5) could be simultaneously obtained as characterizable products in moderate yields, in consequence of the higher reactivity of bis(ethynyl) DHBT than the *meso*-ethynyl OEP. From the ^{1}H NMR spectral studies of their molecular structures, it was suggested that the anisotropy by Ni–OEP ring current effect influences the Th–H located in a deshielded region within the limits of ca. 25 Å. Electronic absorption spectral properties of the OEP–DHBT–OEP system were examined, clearly proving that the orientation of DHBT plays an important role in electronic communications between the two terminal OEP rings. The HH isomer **1** exhibited a broad Soret band, seemingly characteristic of a dimeric property of the 3HTh–OEP system **4**, while the TT isomer **3** split Soret band into two clear bands characteristic of an intensive electronic interaction between the two terminal Ni–OEP rings. In the case of the OEP–$(DHBT)_n$–OEP system, it was indicated that the HH series **17** gradually separate their electronic structures into two main components; the diacetylene-group connected 3HTh–OEP component and the remaining (HH $DHBT)_n$ component. On the other hand, the TT series **18** were tentatively proposed to converge into an electronic structure hybridized between the diacetylene-group connected OEP–(TT DHBT) component and the remaining (TT $DHBT)_n$ component, while retaining their molecular planarities. The electrochemical studies of the OEP–$(DHBT)_n$–OEP system showed that the compounds with $n = 1$ exhibited the higher electron-releasing abilities with increasing the conjugation planarities of DHBT, in order of **1** < **2** < **3**. It was proved that the electron-releasing abilities and electron-transfer processes for the compounds with more than $n = 2$ are also determined by the extension magnitudes of the π-electronic conjugation system, reflecting both of the orientations and numbers of DHBT.

It is also suggested that the OEP–DHBT–OEP system **1**–**3** associates with each other in a highly concentrated solution, reflecting an orientation of DHBT. Continuous investigations of the self-association of **1**–**3**, however, are necessary for an elucidation of the electronic interactions between the two terminal Ni–OEP rings both intra- and intermolecularly, in connection with the self-association effect on their electronic and electrochemical properties.[19]

Experimental

The melting points were determined on a hot-stage apparatus and are uncorrected. EI mass spectra were recorded with a Hitachi RM-50 spectrometer using a direct inlet system and FAB mass spectra with a JEOL AX-505 spectrometer using *m*-nitrobenzyl alcohol (NBA) as a matrix agent. ESI-FT-ICR mass spectra were performed with a Bruker BioAPEX 70e spectrometer equipped

with a 7 T superconducing magnet, using a sample in a solution of $CHCl_3$:MeOH (3:2). IR spectra were measured on a Jasco FT/IR 7300 spectrophotometer as KBr disk or neat sample; only significant absorptions are reported. ^{1}H NMR spectra were measured in $CDCl_3$ and/or THF-d_8 solutions at 25 °C on a JEOL α-400 (400 MHz) spectrometer and were recorded in δ values (/ppm) with TMS as an internal standard. The coupling constants (J) are given in Hz. Electronic absorption spectra were measured on a Shimadzu UV-2200A spectrophotometer; shoulder band is abbreviated as sh. Cyclic voltammetry was performed on a BAS CV-27 potentiometer in CH_2Cl_2 in the presence of n-Bu_4NClO_4 at the scan rate of 120 mV s^{-1}.[22] Silica gel (Fuji Silysia gel BW 820MH or BW 127ZH) and aluminum oxide (CAMAG 504-C-1) were used for column chromatography. CH_2Cl_2 and $CHCl_3$ were distilled over calcium hydride and THF was distilled over sodium ketyl, before use. The reactions were followed by TLC aluminum sheets precoated with Merck silica gel F_{254} or with Merck aluminum oxide GF_{254}. Organic extracts were dried over anhydrous sodium sulfate or magnesium sulfate prior to removal of the solvents. OEP was prepared from methyl 3-oxopentanoate, according to the literature.[31] TMSA and 3HTh were purchased from Tokyo Chemical Industry Co., Ltd.. (Bromomethyl)triphenylphosphonium bromide; Ph_3P^+ $(CH_2Br)Br^-$, dichlorobis(triphenylphosphine)palladium(II); [$PdCl_2(PPh_3)_2$], and [bis(trifluoroacetoxy)iodo]benzene; $C_6H_5I(CF_3COO)_2$ were purchased from Aldrich Chemical Industry Co., Ltd..

5-Ethynyl-2,3,7,8,12,13,17,18-octaethylporphyrinatonickel(II) (9): To a solution of $Ph_3P^+(CH_2Br)Br^-$ (3.52 g, 8.07 mmol) in THF (90 cm^3) was added butyllithium (1.6 M in hexane (1 M = 1 mol dm^{-3}), 5.3 cm^3, 8.48 mmol) dropwise under Ar atmosphere at around 0 °C over 10 min. To the solution, 5-formyl-2,3,7,8,12,13,17,18-octaethylporphyrinatonickel(II)[32] (1.0 g, 1.61 mmol) was added at a time at room temperature and then the resulting mixture was stirred for 2 h. Poured into water, the reaction mixture was extracted with $CHCl_3$, washed with brine, and dried. The residue obtained after removal of the solvent was chromatographed on silica gel (5.2 × 10 cm) with $CHCl_3$:hexane (3:7) to afford the (*E*)-bromovinyl Wittig product[10] (512 mg, 46%) from the first fractions; ^{1}H NMR δ 9.47 (2H, s, *meso*-H), 9.46 (1H, s, *meso*-H), 9.41 (1H, d, J = 14 Hz, OEP–C<u>H</u>=CHBr), 5.47 (1H, d, J = 14 Hz, OEP–CH=C<u>H</u>Br), 3.85–3.79 (16H, m, CH_2), and 1.78–1.64 (24H, m, CH_3) and from the second fractions the (*Z*)-bromovinyl isomer[10] (157 mg, 14%); ^{1}H NMR δ 9.53 (1H, d, J = 7.2 Hz, OEP–C<u>H</u>=CHBr), 9.46 (3H, br s, *meso*-H), 6.85 (1H, d, J = 7.2 Hz, OEP–CH=C<u>H</u>Br), 3.88–3.71 (16H, m, CH_2), and 1.78–1.64 (24H, m, CH_3).

To a solution of sodium hydride (NaH; 60% in oil, 217 mg, 5.45 mmol) and DMSO (0.50 cm^3, 7.06 mmol) in 1,2-dimethoxyethane (120 cm^3) was added the (*E*)- and (*Z*)-bromovinyl compounds (669 mg, 0.96 mmol) in portions.[25] The mixture was stirred under a gentle reflux for 4 h. Poured into iced-water, the reaction mixture was extracted with $CHCl_3$, washed with brine, and dried. The residue obtained after removal of the solvent was chromatographed on alumina (3.6 × 1 cm) with $CHCl_3$:hexane (1:1) to afford the product **9**[10] (545 mg, 92%): Bluish purple powder; ^{1}H NMR δ 9.43 (2H, s, *meso*-H), 9.41 (1H, s, *meso*-H), 4.50 (1H, s, C=CH), 4.46 (4H, q, J = 7.3 Hz, CH_2), 3.84–3.76 (12H, m, CH_2), and 1.78–1.67 (24H, m, CH_3).

3,3′-Dihexyl-5,5′-bis(trimethylsilylethynyl)-2,2′-bithiophene (7): To a mixture of the HH dibromo-DHBT **6**[3a] (1 g, 2.03 mmol), [$PdCl_2(PPh_3)_2$] (148 mg, 0.21 mmol), CuI (22 mg, 0.12 mmol) in diisopropylamine (DIPA; 25 cm^3) was added TMSA (1.33 g, 13.5 mmol) dropwise under Ar atmosphere.[11] The mixture was stirred for 6 h at room temperature. Poured into water, the reaction mixture was extracted with hexane, washed with water, and dried. The residue obtained after removal of the solvent was chromatographed on silica gel (3.2 × 65 cm) with hexane to afford the compound **7** (655 mg, 61%): Yellow oil; MS (EI) m/z 526 (M^+); IR (neat) 2960, 2925, 2855 (CH), 2145 (C≡C), 1250, and 855 cm^{-1}; ^{1}H NMR δ 7.10 (2H, s, Th–H), 2.43 (4H, t, J = 7.4 Hz, CH_2–C_5H_{11}), 1.55–1.20 (16H, CH_2–(CH_2)$_4$–CH_3), 0.87 (6H, t, J = 5.2 Hz, CH_3), and 0.24 (18H, s, $Si(CH_3)_3$); UV (THF) λ_{max} 266 (ε 12600), 307 (24800), and 325 nm (19600, sh). Fiund: C, 68.62; H, 8.91%. Calcd for $C_{30}H_{46}S_2Si_2$: C, 68.38; H, 8.80%.

5,5′-Diethynyl-3,3′-dihexyl-2,2′-bithiophene (8): To a solution of **7** (260 mg, 0.49 mmol) in a mixture of MeOH and hexane (4:1, 6 cm^3) was added anhydrous K_2CO_3 (100 mg, 0.72 mmol). The mixture was stirred for 4 h at room temperature under Ar atmosphere. Quenched with water, the reaction mixture was extracted with hexane, washed with brine, and dried. The residue obtained after removal of the solvent was chromatographed on silica gel (3.2 × 1 cm) with hexane to afford the compound **8** (184 mg, 98%), which decomposes gradually on exposure to light and air. **8**: Colorless oil; MS (EI) m/z 382 (M^+); IR (neat) 3310 (C≡CH), 2960, 2925, 2855 (CH), and 2105 cm^{-1} (C≡C); ^{1}H NMR δ 7.14 (2H, s, Th–H), 3.38 (2H, s, C≡CH), 2.45 (4H, t, J = 7.8 Hz, CH_2–C_5H_{11}), 1.55–1.23 (16H, m, CH_2–(CH_2)$_4$–CH_3), and 0.86 (6H, t, J = 5.4 Hz, CH_3); UV (THF) λ_{max} 240 (ε 11000), 261 (11500), 294 (15700), and 312 nm (13800, sh). Found: C, 75.29; H, 8.19%. Calcd for $C_{24}H_{30}S_2$: C, 75.34; H, 7.90%.

3,3′-Dihexyl-2,5′-bis(trimethylsilylethynyl)-2′,5-bithiophene (11): To a mixture of the HT dibromo-DHBT **10**[3a] (500 mg, 1.02 mmol), [$PdCl_2(PPh_3)_2$] (358 mg, 0.51 mmol), and CuI (78 mg, 0.42 mmol) in DIPA (10 cm^3) was added TMSA (1.20 g, 12.2 mmol) dropwise under Ar atmosphere.[11] The mixture was stirred for 30 h at room temperature. The same procedure as for **7** afforded the compound **11** (415 mg, 77%): Yellow oil; MS (EI) m/z 526 (M); IR (neat) 2960, 2930, 2830 (CH), 2145 (C≡C), 1250, and 855 cm^{-1}; ^{1}H NMR δ 7.04 (1H, s, Th–H), 6.84 (1H, s, Th–H), 2.69–2.64 (4H, m, CH_2–C_5H_{11}), 1.63–1.27 (16H, m, CH_2–(CH_2)$_4$–CH_3), 0.89–0.87 (6H, m, CH_3) and 0.24 (18H, br s, $Si(CH_3)_3$); UV (THF) λ_{max} 230 (ε 13500), 268 (8900), 360 (18700), and 396 nm (10600, sh). Found: C, 68.28; H, 8.73%. Calcd for $C_{30}H_{46}S_2Si_2$: C, 68.38; H, 8.80%.

2,5′-Diethynyl-3,3′-dihexyl-2′,5-bithiophene (12): To a solution of **11** (415 mg, 0.79 mmol) in a mixture of MeOH and hexane (4:1, 15 cm^3) was added anhydrous K_2CO_3 (110 mg, 0.80 mmol). The mixture was stirred for 4 h at room temperature under Ar atmosphere. The same procedure as for **8** afforded the compound **12** (284 mg, 94%), which decomposes gradually on exposure to light and air. **12**: Colorless oil; MS (EI) m/z 382 (M^+); IR (neat) 3310 (C≡CH) and 2100 cm^{-1} (C≡C); ^{1}H NMR δ 7.08 (1H, s, Th–H), 6.86 (1H, s, Th–H), 3.52 (1H, s, C≡CH), 3.38 (1H, s, C≡CH), 2.75–2.67 (4H, m, CH_2–C_5H_{11}), 1.68–1.24 (16H, m, CH_2–(CH_2)$_4$–CH_3), and 0.90–0.83 (6H, m, CH_3); UV (THF) λ_{max} 263 (ε 6900), 348 (20500), and 388 nm (15600, sh). Found: C, 75.29; H, 7.90%, Cakcd for $C_{24}H_{30}S_2$: C, 75.34; H, 7.90%.

3,3′-Dihexyl-2,2′-bis(trimethylsilylethynyl)-5,5′-bithiophene (14): To a mixture of the TT dibromo-DHBT **13**[3a] (475 mg, 0.97 mmol), [$PdCl_2(PPh_3)_2$] (344 mg, 0.49 mmol), and CuI (74 mg, 0.40 mmol) in DIPA (10 cm^3) was added TMSA (1.15 g, 11.6 mmol) dropwise under Ar atmosphere.[11] The mixture was stirred for 50 h at room temperature. The same procedure as for **7** afforded the compound **14** (424 mg, 83%): Yellow oil; MS (EI) m/z 526

(M^+); IR (neat) 2140 (C≡C), 1250, and 845 cm^{-1}; ^1H NMR δ 6.87 (2H, s, Th–H), 2.63 (4H, t, J = 7.8 Hz, CH_2–C_5H_{11}), 1.63–1.27 (16H, m, CH_2–(CH_2)$_4$–CH_3), 0.89 (6H, t, J = 5.5 Hz, CH_3), and 0.25 (18H, s, Si(CH_3)$_3$); UV (THF) λ_{max} 230 (ε 6700), 269 (5400), 355 (16200, sh), 374 (18000), and 395 nm (11400, sh). Found: C, 68.29; H, 8.88%. Calcd for $C_{30}H_{46}S_2Si_2$: C, 68.38; H, 8.80%.

2,2′-Diethynyl-3,3′-dihexyl-5,5′-bithiophene (15): To a solution of **14** (300 mg, 0.57 mmol) in a mixture of MeOH and hexane (4:1, 7.5 cm^3) was added anhydrous K_2CO_3 (78 mg, 0.56 mmol). The mixture was stirred for 4 h at room temperature under Ar atmosphere. The same procedure as for **8** afforded the compound **15** (201 mg, 92%): Colorless oil which decomposes gradually on exposure to light and air; MS (EI) m/z 382 (M^+); IR (neat) 3315 (C≡CH) and 2100 cm^{-1} (C≡C); ^1H NMR δ 6.90 (2H, s, Th–H), 3.50 (2H, s, C≡CH), 2.65 (4H, t, J = 7.7 Hz, CH_2–C_5H_{11}), 1.63–1.30 (16H, m, CH_2–(CH_2)$_4$–CH_3), and 0.89 (6H, t, J = 5.5 Hz, CH_3); UV (THF) λ_{max} 263 (ε 6600), 345 (17800, sh), 360 (18600), and 383 nm (12100, sh). Found: C, 75.26; H, 8.03%. Calcd for $C_{24}H_{30}S_2$: C, 75.34; H, 7.90%.

2-Bromo-3-hexyl-5-(trimethylsilylethynyl)thiophene (20): To a mixture of TMSA (210 mg, 1.53 mmol) and 2,5-dibromo-3-hexylthiophene (**19**)[2] (500 mg, 1.53 mmol) in DIPA (5.0 cm^3) were added [$PdCl_2(PPh_3)_2$] (54 mg, 0.077 mmol) and CuI (7.3 mg, 0.039 mmol) with stirring under Ar atmosphere.[11] The mixture was stirred for 4 h at room temperature. The same procedure as for **7** afforded the compound **20** (308 mg, 59%): Pale yellow oil; MS (EI) m/z 342 (M^+) and 344 (M^+ + 2) based on ^{79}Br; IR (neat) 2960, 2930, 2860 (CH), 2145 (C≡C), 1250, and 845 cm^{-1}; ^1H NMR δ 6.92 (1H, s, Th–H), 2.49 (2H, t, J = 7.6 Hz, CH_2–C_5H_{11}), 1.55–1.28 (8H, m, CH_2–(CH_2)$_4$–CH_3), 0.88 (3H, t, J = 5.3 Hz, CH_3), and 0.23 (9H, s, Si(CH_3)$_3$); UV (THF) λ_{max} 263 (ε 7650), 291 (14100), and 305 nm (11500, sh). Found: C, 52.55; H, 6.77%. Calcd for $C_{15}H_{23}BrSSi$: C, 52.48; H, 6.71%.

2-Bromo-5-ethynyl-3-hexylthiophene (21): To a solution of **20** (308 mg, 0.90 mmol) in dry MeOH (1.5 cm^3) was added anhydrous K_2CO_3 (131 mg, 0.95 mmol). The mixture was stirred for 4 h at room temperature under Ar atmosphere. The same procedure as for **8** afforded the compound **21** (238 mg, 98%), which decomposes gradually on exposure to light and air. **21**: Colorless oil; MS (EI) m/z 270 (M^+) and 272 (M^+ + 2) based on ^{79}Br; IR (neat) 3310 (C≡CH), 2955, 2930, 2855 (CH), and 2105 cm^{-1} (C≡C); ^1H NMR δ 6.96 (1H, s, Th–H), 3.35 (1H, s, C≡CH), 2.51 (2H, t, J = 7.3 Hz, CH_2–C_5H_{11}), 1.60–1.26 (8H, m, CH_2–(CH_2)$_4$–CH_3), and 0.89 (3H, t, J = 5.3 Hz, CH_3); UV (THF) λ_{max} 252 (ε 9000), 258 (9500), and 282 nm (13300). Found: C, 52.98; H, 5.75%. Calcd for $C_{12}H_{15}BrS$: C, 53.14; H, 5.54%.

3-Hexyl-2-iodothiophene (22): To a solution of 3HTh (1.68 g, 10 mmol) in CCl_4 (12.5 cm^3) were added I_2 (1.27 g, 5 mmol) and $C_6H_5I(CF_3COO)_2$ (2.37 g, 5.55 mmol).[13b] The mixture was stirred for 5 h at room temperature. After the solvent was removed under reduced pressure, the residue was passed through a short column of silica gel (3.2 × 10 cm) and the fractions eluted with hexane were collected. Distillation of the residue after removal of solvent, bp 65–66 °C/532 Pa (1 mmHg = 133 Pa), afforded the compound **22**[13] (1.70 g, 58%): Colorless oil; MS (EI) m/z 294 (M^+); IR (neat) 2955, 2925, and 2855 cm^{-1} (CH); ^1H NMR δ 7.37 (1H, d, J = 5.3 Hz, Th–H), 6.75 (1H, d, J = 5.3 Hz, Th–H), 2.55 (2H, t, J = 7.1 Hz, CH_2–C_5H_{11}), 1.55–1.31 (8H, m, CH_2–(CH_2)$_4$–CH_3), and 0.88 (3H, t, J = 5.2 Hz, CH_3); UV (THF) λ_{max} 245 nm (ε 8120). Found: C, 40.84; H, 5.13%. Calcd for $C_{10}H_{15}IS$: C, 40.83; H, 5.14%.

3-Hexyl-2-(trimethylsilylethynyl)thiophene (23): To a mixture of TMSA (114 mg, 1.16 mmol) and **22** (285 mg, 0.97 mmol) in DIPA (3.0 cm^3) were added [$PdCl_2(PPh_3)_2$] (48 mg, 0.07 mmol) and CuI (6.7 mg, 0.03 mmol) with stirring under Ar atmosphere.[11] The mixture was stirred for 4 h at room temperature. The same procedure as for **7** afforded the compound **23** (232 mg, 90%): Pale yellow oil; MS (EI) m/z 264 (M^+); IR (neat) 2960, 2930, 2860 (CH), 2145 (C≡C), 1250, and 845 cm^{-1}; ^1H NMR δ 7.12 (1H, d, J = 5.1 Hz, Th–H), 6.82 (1H, d, J = 5.1 Hz, Th–H), 2.69 (2H, t, J = 7.3 Hz, CH_2–C_5H_{11}), 1.63–1.31 (8H, m, CH_2–(CH_2)$_4$–CH_3), 0.87 (3H, t, J = 5.2 Hz, CH_3), and 0.25 (9H, s, Si(CH_3)$_3$); UV (THF) λ_{max} 210 (ε 8120), 268 (12500), and 276 nm (12900). Found: C, 68.17; H, 9.05%. Calcd for $C_{15}H_{24}SSi$: C, 68.11; H, 9.15%.

2-Ethynyl-3-hexylthiophene (24): To a solution of **23** (100 mg, 0.38 mmol) in dry MeOH (1 cm^3) was added anhydrous K_2CO_3 (57 mg, 0.41 mmol). The mixture was stirred for 4 h at room temperature under Ar atmosphere. The same procedure as for **8** afforded the compound **24**[8] (70 mg, 96%), which decomposes gradually on exposure to light and air. **24**: Colorless oil; MS (EI) m/z 192 (M^+); IR (neat) 3310 (C≡CH), 2955, 2930, 2860 (CH), and 2100 cm^{-1} (C≡C); ^1H NMR δ 7.15 (1H, d, J = 5.3 Hz, Th–H), 6.84 (1H, d, J = 5.3 Hz, Th–H), 3.42 (1H, s, C≡CH), 2.71 (2H, t, J = 7.3 Hz, CH_2–C_5H_{11}), 1.63–1.31 (8H, m, CH_2–(CH_2)$_4$–CH_3), and 0.88 (3H, t, J = 5.3 Hz, CH_3); UV (THF) λ_{max} 262 nm (ε 9240). Found: C, 75.25; H, 8.51%. Calcd for $C_{12}H_{16}S$: C, 75.00; H, 8.33%.

5,5′-[3,3′-Dihexyl-2,2′-bithiophene-5,5′-diylbis(1,3-butadiyne-1,4-diyl)]bis[2,3,7,8,12,13,17,18-octaethylporphyrinato-nickel(II)] (1): To a solution of $Cu(OAc)_2$ (1.34 g, 7.38 mmol) in a mixture of pyridine:MeOH (5:1, 48 cm^3) was added a solution of **8** (85 mg, 0.22 mmol) and **9** (300 mg, 0.49 mmol) in a mixture of pyridine:MeOH (5 :1, 260 cm^3) dropwise at 40 °C over 24 h.[12] The mixture was stirred at 40 °C for further 24 h. Poured into iced-water, the reaction mixture was extracted with $CHCl_3$. The extracts were washed with water, shaked with dil. HCl, washed with water, shaked with sat. $NaHCO_3$ aq, washed with water successively, and then dried. The residue after removal of the solvents was chromatographed on silica gel (3.2 × 60 cm). Elutions with $CHCl_3$–hexane (6:1) gave a mixture of the OEP–(DHBT)$_n$–OEP system **17** from the first fractions and the diacetylene-group connected OEP dimer **16**[10] (94 mg, 31% based on **9**) from the second fractions. Then, the mixture of **17** was again chromatographed on silica gel (3.2 × 60 cm) with $CHCl_3$–hexane (1:1) to afford each compound; n = 5 (6 mg, 4% based on **8**), n = 4 (10 mg, 7% based on **8**), n = 3 (17 mg, 10% based on **8**), n = 2 (30 mg, 13% based on **8**), and n = 1 (**1**; 52 mg, 15% based on **8**) in order.

1: Black-purple fine needles ($CHCl_3$–MeOH); Mp > 300 °C (dec); MS (FAB) m/z 1608 (M^+ + 1); IR (KBr) 2960, 2925, 2870 (CH), 2145, and 2125 cm^{-1} (C≡C); ^1H NMR ($CDCl_3$) δ 9.42 (4H, s, *meso*-H), 9.40 (2H, s, *meso*-H), 7.33 (2H, s, Th–H), 4.12 (8H, q, J = 7.3 Hz, OEP–CH_2), 3.84–3.75 (24H, m, OEP–CH_2), 2.55 (4H, t, J = 7.4 Hz, Th–CH_2–C_5H_{11}), 1.82–1.71 (42H, m, OEP–CH_3), 1.31–1.25 (16H, m, Th–CH_2–(CH_2)$_4$–CH_3), and 0.89 (12H, q, J = 6.7 Hz, OEP–CH_3). ^1H NMR (THF-d_8) δ 9.51 (4H, s, *meso*-H), 9.49 (2H, s, *meso*-H), 7.47 (2H, s, Th–H), 4.17 (8H, q, J = 7.3 Hz, OEP–CH_2), 3.89–3.81 (24H, m, OEP–CH_2), 2.61 (4H, t, J = 7.4 Hz, Th–CH_2–C_5H_{11}), 1.86–1.75 (48H, m, OEP–CH_3), 1.35–1.28 (16H, m, Th–CH_2–CH_2–(CH_2)$_4$–CH_3), and 0.93 (6H, q, J = 5.6 Hz, Th–CH_2–(CH_2)$_4$–CH_2); UV-vis ($CHCl_3$) λ_{max} 328 (ε 32700), 440 (182000, sh), 454 (190000), 562 (24500, sh), and 593 nm

(28000). Found: C, 74.55; H, 7.29; N, 6.68%. Calcd for $C_{100}H_{114}N_8Ni_2S_2$: C, 74.62; H, 7.14; N 6.96%.

Selected physical data for the compounds of type **17** are shown in order to ascertain their structures. The further structural properties will be reported elsewhere in more detail. ***n*** = **2**: Black powder ($CHCl_3$–MeOH); Mp > 300 °C; MS (ESI-FT-ICR) *m*/2*z* 993.93665 (M^+); IR (KBr) 2960, 2925, 2870 (CH), 2150, and 2125 cm^{-1} (C≡C); ^1H NMR (THF-d_8) δ 9.48 (4H, s, *meso*-H), 9.46 (2H, s, *meso*-H), 7.44 (2H, s, Th–H), 7.37 (2H, s, Th–H), 4.16 (8H, q, J = 6.6 Hz, OEP–CH_2), 3.87–3.78 (24H, m, OEP–CH_2), 2.57–2.51 (8H, m, Th–CH_2–C_5H_{11}), 1.84–1.24 (80H, m, Th–CH_2–(CH_2)$_4$–CH_3 and OEP–CH_3), and 0.92–0.86 (12H, t m, Th–CH_2–$(CH_2)_4$–CH_3); UV-vis ($CHCl_3$) λ_{max} 330 (ε 33000), 450 (200000), 562 (20500, sh), 593 (24000), and 613 nm (19500, sh). ***n*** = **3**: Black powder ($CHCl_3$–MeOH); Mp > 260 °C; MS (ESI-FT-ICR) *m*/2*z* 1183.99047 (M^+); IR (KBr) 2960, 2925, 2860 (CH), 2145, and 2125 cm^{-1} (C≡C); ^1H NMR (THF-d_8) δ 9.49 (4H, s, *meso*-H), 9.47 (2H, s, *meso*-H), 7.44 (2H, s, Th–H), 7.38 (2H, s, Th–H), 7.36 (2H, s, Th–H), 4.16 (8H, q, J = 7.6 Hz, OEP–CH_2), 3.88–3.79 (24H, m, OEP–CH_2), 2.58–2.49 (12H, m, Th–CH_2–C_5H_{11}), 1.86–1.25 (96H, m, Th–CH_2–(CH_2)$_4$–CH_3 and OEP–CH_3), and 0.90–0.86 (18H, t m, Th–CH_2–$(CH_2)_4$–CH_3); UV-vis ($CHCl_3$) λ_{max} 350 (ε 46000, sh), 375 (60500, sh), 448 (209000), 565 (19000, sh), 589 (25000), and 615 nm (16500, sh). ***n*** = **4**: Black powder ($CHCl_3$–MeOH); Mp > 260 °C; MS (ESI-FT-ICR) *m*/3*z* 916.08107 (M^+); IR (KBr) 2960, 2925, 2855 (CH), 2145, and 2125 cm^{-1} (C≡C); ^1H NMR (THF-d_8) δ 9.49 (4H, s, *meso*-H), 9.47 (2H, s, *meso*-H), 7.44 (2H, s, Th–H), 7.38 (2H, s, Th–H), 7.36 (4H, s, Th–H), 4.15 (8H, q, J = 7.3 Hz, OEP–CH_2), 3.86–3.79 (24H, m, OEP–CH_2), 2.57–2.47 (16H, m, Th–CH_2–C_5H_{11}), 1.83–1.27 (112H, m, Th–CH_2–(CH_2)$_4$–CH_3 and OEP–CH_3), and 0.90–0.85 (24H, t m, Th–CH_2–$(CH_2)_4$–CH_3); UV-vis ($CHCl_3$) λ_{max} 364 (ε 75000, sh), 394 (105000, sh), 447 (218000), 563 (18000, sh), 590 (21900), and 613 nm (17500, sh). ***n*** = **5**: Black powder ($CHCl_3$–MeOH); Mp > 230 °C; MS (ESI-FT-ICR) *m*/3*z* 1042.77929 (M^+); IR (KBr) 2960, 2925, 2860 (CH), 2145, and 2125 cm^{-1} (C≡C); ^1H NMR (THF-d_8) δ 9.50 (4H, s, *meso*-H), 9.48 (2H, s, *meso*-H), 7.45 (2H, s, Th–H), 7.38 (2H, s, Th–H), 7.37 (6H, br s, Th–H), 4.15 (8H, q, J = 7.3 Hz, OEP–CH_2), 3.88–3.80 (24H, m, OEP–CH_2), 2.58–2.47 (20H, m, Th–CH_2–C_5H_{11}), 1.83–1.26 (128H, m, Th–CH_2–(CH_2)$_4$–CH_3 and OEP–CH_3), and 0.90–0.85 (30H, t m, Th–CH_2–$(CH_2)_4$–CH_3); UV-vis ($CHCl_3$) λ_{max} 365 (ε 98000, sh), 395 (130000, sh), 447 (245000), 565 (38000, sh), 589 (22000), and 615 nm (16000, sh).

5,5′-[3,3′-Dihexyl-2′,5-bithiophene-2′,5-diylbis(1,3-butadiyne-1,4-diyl)]bis[2,3,7,8,12,13,17,18-octaethylporphyrinatonickel(II)] (2): To a solution of $Cu(OAc)_2$ (690 mg, 3.80 mmol) in a mixture of pyridine:MeOH (5:1, 18 cm^3) was added a solution of **12** (26 mg, 0.068 mmol) and **9** (162 mg, 0.26 mmol) in a mixture of pyridine:MeOH (5:1, 108 cm^3) dropwise at 40 °C over 24 h.[12] The mixture was stirred at 40 °C for further 24 h. After the usual work-up, the residue was chromatographed on silica gel (3.2 × 60 cm). The fractions eluted with $CHCl_3$–hexane (3:7) afforded the compound **2** (29 mg, 26% based on **12**) and the OEP dimer **16**[10] (54 mg, 36% based on **9**), successively.

2: Black-purple fine needles ($CHCl_3$–MeOH); Mp > 300 °C (dec); MS (FAB) *m*/*z* 1608 (M^+ + 1); IR (KBr) 2960, 2930, 2870 (CH), 2150, and 2130 cm^{-1} (C≡C); ^1H NMR ($CDCl_3$) δ 9.42 (4H, br s, *meso*-H), 9.39 (2H, s, *meso*-H), 7.24 (1H, s, Th–H), 6.99 (1H, s, Th–H), 4.17–4.10 (8H, q m, OEP–CH_2), 3.82–3.76 (24H, m, OEP–CH_2), 2.83–2.76 (4H, t m, Th–CH_2–C_5H_{11}), 1.83–1.35 (64H, m, OEP–CH_3 and Th–CH_2–(CH_2)$_4$–CH_3), and 0.92–0.89 (6H, t m, Th–CH_2–$(CH_2)_4$–CH_3). ^1H NMR (THF-d_8) δ 9.50 (4H, br s, *meso*-H), 9.48 (2H, s, *meso*-H), 7.39 (1H, s, Th–H), 7.16 (1H, s, Th–H), 4.19 (4H, t, J = 6.6 Hz, OEP–CH_2), 4.16 (4H, t, J = 6.6 Hz, OEP–CH_2), 3.89–3.80 (24H, m, OEP–CH_2), 2.87–2.80 (4H, t m, Th–CH_2–C_5H_{11}), 1.86–1.36 (64H, m, OEP–CH_3 and Th–CH_2–(CH_2)$_2$–CH_3), and 0.94–0.87 (6H, t m, Th–CH_2–$(CH_2)_4$–CH_3); UV-vis ($CHCl_3$) λ_{max} 330 (ε 22000), 440 (146000), 471 (133000), 562 (25000, sh), and 600 nm (43000). Found: C, 74.38; H, 7.48; N, 6.70%. Calcd for $C_{100}H_{114}N_8Ni_2S_2$: C, 74.62; H, 7.14; N 6.96%.

From the fractions prior to those of **2**, the by-product (7 mg, 5.2% based on **12**) was also obtained; it was found to be a mixture of two or three isomers bearing the two DHBT moieties, on the bases of MS and ^1H NMR spectral measurements. MS (ESI-FT-ICR) *m*/2*z* complicated peaks at around 994 (M^+); ^1H NMR ($CDCl_3$) δ 9.42 (total 4H, br s, *meso*-H), 9.39 (total 2H, br s, *meso*-H), 7.22, 7.16, 6.96, 6.94, 6.93 (total 4H, each s, Th–H), 4.17–4.09 (total 8H, m, OEP–CH_2), 3.81–3.76 (total 24H, m, OEP–CH_2), 2.82–2.70 (total 8H, m, Th–CH_2–C_5H_{11}), 1.83–1.26 (total 80H, m, OEP–CH_3 and Th–CH_2–(CH_2)$_4$–CH_3), and 0.92–0.89 (total 6H, m, Th–CH_2–$(CH_2)_4$–CH_3). Separation of the mixture to each isomer by means of preparative TLC and HPLC was unsuccessful, because of the high similarity in their physicochemical properties.

5,5′-[3,3′-Dihexyl-5′,5′-bithiophene-2,2′-diylbis(1,3-butadiyne-1,4-diyl)]bis[2,3,7,8,12,13,17,18-octaethylporphyrinatonickel(II)] (3): To a solution of $Cu(OAc)_2$ (427 mg, 2.35 mmol) in a mixture of pyridine:MeOH (5:1, 18 cm^3) was added a solution of **15** (183 mg, 0.48 mmol) and **9** (650 mg, 1.06 mmol) in a mixture of pyridine:MeOH (5:1, 90 cm^3) dropwise at 40 °C over 6 h.[12] The mixture was stirred at 40 °C for further 3 h. After the usual work-up, the residue was chromatographed on silica gel (3.2 × 40 cm). Elutions with $CHCl_3$–hexane (6:1) gave a mixture of the OEP–$(DHBT)_n$–OEP system **18** from the first fractions and the diacetylene-group connected OEP dimer **16**[10] (138 mg, 21% based on **9**) from the second fractions. Then, the mixture of **18** was again chromatographed on silica gel (3.2 × 60 cm) with $CHCl_3$–hexane (2:3) to afford each compound; n = 5 (32 mg, 11% based on **15**), n = 4 (26 mg, 8% based on **15**), n = 3 (100 mg, 26% based on **15**), n = 2 (78 mg, 16% based on **15**), and n = 1 (**3**; 155 mg, 20% based on **15**) in order.

3: Black-purple fine needles ($CHCl_3$–MeOH); Mp > 300 °C (dec); MS (FAB) *m*/*z* 1608 (M^+ + 1); IR (KBr) 2960, 2925, 2865 (CH), 2145, and 2125 cm^{-1} (C≡C); ^1H NMR ($CDCl_3$) δ 9.42 (4H, s, *meso*-H), 9.39 (2H, s, *meso*-H), 7.00 (1H, s, Th–H), 4.14 (8H, q, J = 7.6 Hz, OEP–CH_2), 3.86–3.76 (24H, m, OEP–CH_2), 2.79 (4H, t, J = 7.6 Hz, Th–CH_2–C_5H_{11}), 1.83–1.72 (42H, m, OEP–CH_3), 1.44–1.25 (16H, m, Th–CH_2–(CH_2)$_4$–CH_3), and 0.91 (12H, q, J = 6.6 Hz, Th–CH_2–$(CH_2)_4$–CH_3). ^1H NMR (THF-d_8) δ 9.51 (4H, s, *meso*-H), 9.48 (2H, s, *meso*-H), 7.25 (2H, s, Th–H), 4.18 (8H, t, J = 7.6 Hz, OEP–CH_2), 3.89–3.81 (24H, m, OEP–CH_2), 2.84 (4H, t, J = 7.6 Hz, Th–CH_2–C_5H_{11}), 1.85–1.29 (64H, m, Th–CH_2–(CH_2)$_4$–CH_3 and OEP–CH_3), and 0.92 (6H, q, J = 6.6 Hz, Th–CH_2–$(CH_2)_4$–CH_3); UV-vis ($CHCl_3$) λ_{max} 340 (ε 28000, sh), 440 (57500, sh), 441 (134000), 484 (143000), 562 (27500, sh), and 601 nm (52000). Found: C, 74.44; H, 7.41; N, 6.71%. Calcd for $C_{100}H_{114}N_8Ni_2S_2$: C, 74.62; H, 7.14; N 6.96%.

Selected physical data for the compounds of type **18** are shown in order to ascertain their structures. The further structural properties will be reported elsewhere. ***n*** = **2**: Black powder ($CHCl_3$–MeOH); Mp > 300 °C; MS (ESI-FT-ICR) *m*/2*z* 993.94776 (M^+); IR (KBr) 2960, 2925, 2870 (CH), 2150, and 2125 cm^{-1} (C≡C); ^1H NMR (THF-d_8) δ 9.51 (4H, s, *meso*-H), 9.49 (2H, s, *meso*-H),

7.24 (2H, s, Th–H), 7.22 (2H, s, Th–H), 4.18 (8H, q, J = 6.6 Hz, OEP–CH_2), 3.89–3.81 (24H, m, OEP–CH_2), 2.83 (4H, t, J = 7.6 Hz, Th–CH_2–C_5H_{11}), 2.75 (4H, t, J = 7.5 Hz, Th–CH_2–C_5H_{11}), 1.85–1.29 (80H, m, Th–CH_2–(CH_2)$_4$–CH_3 and OEP–CH_3), and 0.93–0.90 (12H, t m, Th–CH_2–$(CH_2)_4$–CH_3); UV-vis ($CHCl_3$) λ_{max} 350 (ε 44500, sh), 446 (169000), 483 (196000), 562 (3500, sh), and 597 nm (56000). ***n* = 3**: Black powder ($CHCl_3$–MeOH); Mp > 280 °C; MS (ESI-FT-ICR) $m/3z$ 789.01384 (M^+); IR (KBr) 2960, 2925, 2855 (CH), 2150, and 2125 cm^{-1} (C≡C); ^{1}H NMR (THF-d_8) δ 9.51 (4H, s, *meso*-H), 9.49 (2H, s, *meso*-H), 7.24 (2H, s, Th–H), 7.22 (2H, s, Th–H), 7.20 (2H, s, Th–H), 4.17 (8H, q, J = 7.6 Hz, OEP–CH_2), 3.89–3.81 (24H, m, OEP–CH_2), 2.83 (4H, t, J = 7.6 Hz, Th–CH_2–C_5H_{11}), 2.76–2.71 (8H, m, Th–CH_2–C_5H_{11}), 1.85–1.29 (96H, m, Th–CH_2–(CH_2)$_4$–CH_3 and OEP–CH_3), and 0.93–0.89 (18H, t m, Th–CH_2–$(CH_2)_4$–CH_3); UV-vis ($CHCl_3$) λ_{max} 350 (ε 35500, sh), 405 (78000, sh), 442 (162000, sh), 483 (198000), 565 (28500, sh), and 595 nm (44600). ***n* = 4**: Black powder ($CHCl_3$–MeOH); Mp > 250 °C; MS (ESI-FT-ICR) $m/2z$ 1373.60673 (M^+); IR (KBr) 2960, 2925, 2855 (CH), 2150, and 2125 cm^{-1} (C≡C); ^{1}H NMR (THF-d_8) δ 9.51 (4H, s, *meso*-H), 9.49 (2H, s, *meso*-H), 7.24 (2H, s, Th–H), 7.22 (2H, s, Th–H), 7.20 (4H, s, Th–H), 4.18 (8H, q, J = 7.3 Hz, OEP–CH_2), 3.89–3.81 (24H, m, OEP–CH_2), 2.83 (4H, t, J = 7.6 Hz, Th–CH_2–C_5H_{11}), 2.76–2.71 (12H, m, Th–CH_2–C_5H_{11}), 1.85–1.29 (112H, m, Th–CH_2–(CH_2)$_4$–CH_3 and OEP–CH_3), and 0.93–0.89 (24H, t m, Th–CH_2–$(CH_2)_4$–CH_3); UV-vis ($CHCl_3$) λ_{max} 350 (ε 39000, sh), 405 (75000, sh), 443 (164000, sh), 482 (203000), 560 (4000, sh), and 594 nm (40000). ***n* = 5**: Black powder ($CHCl_3$–MeOH); Mp > 250 °C; MS (ESI-FT-ICR) $m/3z$ 1042.46152 (M^+); IR (KBr) 2960, 2925, 2850 (CH), 2145, and 2125 cm^{-1} (C≡C); ^{1}H NMR (THF-d_8) δ 9.51 (4H, s, *meso*-H), 9.49 (2H, s, *meso*-H), 7.24 (2H, s, Th–H), 7.21 (2H, s, Th–H), 7.19 (6H, br s, Th–H), 4.18 (8H, q, J = 7.3 Hz, OEP–CH_2), 3.89–3.81 (24H, m, OEP–CH_2), 2.83 (4H, t, J = 7.6 Hz, Th–CH_2–C_5H_{11}), 2.76–2.70 (16H, m, Th–CH_2–C_5H_{11}), 1.85–1.29 (134H, m, Th–CH_2–(CH_2)$_4$–CH_3 and OEP–CH_3), and 0.93–0.87 (24H, t m, Th–CH_2–$(CH_2)_4$–CH_3); UV-vis ($CHCl_3$) λ_{max} 350 (ε 40500, sh), 443 (168000, sh), 482 (210000), 560 (24000, sh), and 594 nm (36000).

5-[4-(3-Hexyl-2-thienyl)-1,3-butadiyne-1-yl]-2,3,7,8,12,13, 17,18-octaethylporphyrinatonickel(II)] (4): To a solution of $Cu(OAc)_2$ (1.40 g, 7.71 mmol) in a mixture of pyridine:MeOH (5:1, 48 cm^3) was added a solution of **21** (238 mg, 0.88 mmol) and **9** (53 mg, 0.088 mmol) in a mixture of pyridine:MeOH (5:1, 190 cm^3) dropwise at 40 °C over 10 h.[12] The mixture was stirred at 40 °C for further 38 h. After the usual work-up, the residue was chromatographed on silica gel (3.2 × 28 cm). The fractions eluted with hexane afforded 2,2′-dibromo-3,3′-dihexyl-5,5′-(1,3-butadiyne-1,4-diyl)bithiophene (**26**) (140 mg, 59% based on **21**): Reddish yellow oil; MS (EI) m/z 538 (M^+), 540 (M^+ + 2), and 542 (M^+ + 4) based on ^{79}Br; IR (KBr) 2955, 2930, 2855 (CH), 2195, and 2140 cm^{-1} (C≡C); ^{1}H NMR δ 7.02 (2H, s, Th–H), 2.52 (4H, t, J = 6.6 Hz, CH_2–C_5H_{11}), 1.63–1.18 (16H, m, CH_2–(CH_2)$_4$–CH_3), and 0.86 (6H, t, J = 5.4 Hz, CH_2–$(CH_2)_4$–CH_3); UV-vis (THF) λ_{max} 248 (ε 19900), 274 (18000), 314 (26500), 332 (24500), 353 (28400), and 379 nm (21800). Found: C, 53.10; H, 5.38%. Calcd for $C_{24}H_{28}Br_2S_2$: C, 53.33; H, 5.18%. The later fractions eluted with $CHCl_3$–hexane (3:7) afforded the bromo derivative **25** (44 mg, 57% based on **21**): Bluish purple fine needles ($CHCl_3$–MeOH); Mp > 230 °C (dec); MS m/z 883 (M^+) and 885 (M^+ + 2) based on ^{79}Br; IR (KBr) 2965, 2930, 2870 (CH), 2180, and 2130 cm^{-1} (C≡C); ^{1}H NMR δ 9.41 (2H, s, *meso*-H), 9.39 (1H, s, *meso*-H), 7.10 (1H, s, Th–H), 4.11 (4H, q, J = 7.3 Hz, OEP–CH_2), 3.83–3.74 (12H, m, OEP–CH_2), 2.54 (2H, t, J = 7.6 Hz, Th–CH_2–C_5H_{11}), 1.81–1.70 (24H, m, OEP–CH_3), 1.60–1.25 (8H, m, Th–CH_2–(CH_2)$_4$–CH_3), and 0.90 (3H, t, J = 5.5 Hz, Th–CH_2–$(CH_2)_4$–CH_3); UV-vis ($CHCl_3$) λ_{max} 445 (ε 135000), 583 (13500), and 605 nm (12400). Found: C, 74.44; H, 7.53; N, 6.58%. Calcd for $C_{50}H_{57}BrN_4NiS$: C, 67.95; H, 6.45, N, 6.34%. From the later fractions eluted with $CHCl_3$–hexane (2:3) a very small amount of **16**[10] was obtained.

To a solution of **25** (40 mg, 0.045 mmol) in THF (30 cm^3) was added $LiAlH_4$ (26 mg, 0.68 mmol) at a time at 0 °C. The mixture was stirred 3 h at room temperature. After addition of ethyl acetate (0.5 cm^3), the reaction mixture was poured into water and extracted with $CHCl_3$. The extracts were washed with brine and dried. The residue was chromatographed on silica gel (2.5 × 5 cm) with $CHCl_3$ to afford the compound **4** (34.8 mg, 96%): Bluish purple fine needles ($CHCl_3$–MeOH); Mp > 220 °C (dec); MS (FAB) m/z 806 (M^+ + 1); IR (KBr) 2965, 2930, 2870 (CH), 2190, and 2135 cm^{-1} (C≡C); ^{1}H NMR ($CDCl_3$) δ 9.41 (2H, s, *meso*-H), 9.39 (1H, s, *meso*-H), 7.25 (1H, s, Th–H), 6.95 (1H, s, Th–H), 4.12 (4H, q, J = 7.6 Hz, OEP–CH_2), 3.83–3.76 (12H, m, OEP–CH_2), 2.60 (2H, t, J = 7.5 Hz, Th–CH_2–C_5H_{11}), 1.81–1.60 (24H, m, OEP–CH_3), 1.31–1.25 (8H, m, Th–CH_2–(CH_2)$_4$–CH_3), and 0.90 (3H, t, J = 5.8 Hz, Th–CH_2–$(CH_2)_4$–CH_3). ^{1}H NMR (THF-d_8) δ 9.49 (2H, s, *meso*-H), 9.47 (1H, s, *meso*-H), 7.34 (1H, s, Th–H), 7.14 (1H, s, Th–H), 4.15 (4H, q, J = 7.6 Hz, OEP–CH_2), 3.88–3.80 (12H, m, OEP–CH_2), 2.61 (2H, t, J = 7.5 Hz, Th–CH_2–C_5H_{11}), 1.82–1.62 (24H, m, OEP–CH_3), 1.33–1.28 (8H, m, Th–CH_2–(CH_2)$_4$–CH_3), and 0.89 (3H, t, J = 5.8 Hz, Th–CH_2–$(CH_2)_4$–CH_3); UV-vis ($CHCl_3$) λ_{max} 443 (ε 149000), 574 (12000), and 603 nm (12500). Found: C, 74.25; H, 7.50; N, 6.68%. Calcd for $C_{50}H_{58}N_4NiS$: C, 74.53; H, 7.26; N, 6.95%.

5-[4-(4-Hexyl-2-thienyl)-1,3-butadiyne-1-yl]-2,3,7,8,12,13, 17,18-octaethylporphyrinatonickel(II)] (5): To a solution of $Cu(OAc)_2$ (852 mg, 4.69 mmol) in a mixture of pyridine:MeOH (5:1, 30 cm^3) was added a solution of **24** (137 mg, 0.71 mmol) and **9** (43 mg, 0.070 mmol) in a mixture of pyridine:MeOH (5 :1, 156 cm^3) dropwise at 40 °C over 6 h.[12] The mixture was stirred at 40 °C overnight. After the usual work-up, the residue was chromatographed on silica gel (3.2 × 23 cm). The fractions eluted with $CHCl_3$–hexane (1:9) afforded 3,3′-dihexyl-2,2′-(1,3-butadiyne-1,4-diyl)bithiophene[8] (**27**) (109 mg, 80% based on **24**): Yellow oil; MS (EI) m/z 382 (M^+); IR (KBr) 2925, 2855 (CH), and 2135 cm^{-1} (C≡C); ^{1}H NMR δ 7.20 (1H, d, J = 5.1 Hz, Th–H), 6.87 (1H, d, J = 5.1 Hz, Th–H), 2.74 (4H, t, J = 6.5 Hz, CH_2–C_5H_{11}), 1.70–1.33 (16H, m, CH_2–(CH_2)$_4$–CH_3), and 0.95–0.82 (6H, m, CH_3); UV (THF) λ_{max} 227 (ε 12000), 247 (15300), 265 (10700, sh), 277 (5100), 291 (2400), 321 (14900, sh), 340 (18700), and 368 nm (14800). Found: C, 75.60; H, 8.10%. Calcd for $C_{24}H_{30}S_2$: C, 75.34; H, 7.90%.

The later fractions eluted with $CHCl_3$–hexane (1:4) afforded the product **5** (23 mg, 41% based on **9**): Bluish purple fine needles ($CHCl_3$–MeOH); Mp > 240 °C (dec); MS m/z (FAB) 806 (M^++ 1); IR (neat) 2965, 2930, 2870 (CH), 2185, and 2130 cm^{-1} (C≡C); ^{1}H NMR δ 9.42 (2H, s, *meso*-H), 9.39 (1H, s, *meso*-H), 7.24 (1H, d, J = 5.2 Hz, Th–H), 6.91 (1H, d, J = 5.2 Hz, Th–H), 4.13 (4H, q, J = 7.4 Hz, OEP–CH_2), 3.84–3.75 (12H, m, OEP–CH_2), 2.82 (2H, t, J = 7.5 Hz, Th–CH_2–C_5H_{11}), 1.82–1.66 (24H, m, OEP–CH_3), 1.40–1.33 (8H, m, Th–CH_2–(CH_2)$_4$–CH_3), and 0.89 (3H, t, J = 5.3 Hz, Th–CH_2–$(CH_2)_4$–CH_3); UV-vis ($CHCl_3$) λ_{max} 281 (ε 21200), 331 (17200), 446 (145000), 572 (12200), and 602 nm (12300). Found: C, 74.33; H, 7.55; N, 6.85%. Calcd for $C_{50}H_{58}N_4NiS$: C, 74.53; H, 7.26, N, 6.95%. From the later frac-

tions eluted with $CHCl_3$–hexane (2:3) was obtained a small amount of **16**[10].

Financial support by a Grant-in-Aid for Scientific Research No. 11640528 from the Ministry of Education, Science, Sports and Culture, is gratefully acknowledged.

References

1 D. Yu, A. Gharavi, and L. Yu, *J. Am. Chem. Soc.*, **117**, 11680 (1995); R. Wu, J. S. Schumm, D. L. Pearson, and J. M. Tour, *J. Org. Chem.*, **61**, 6906 (1996); Y. Greenwald, G. Cohen, J. Poplawski, E. Ehrenfreund, S. Speiser, and D. Davidov, *J. Am. Chem. Soc.*, **118**, 2980 (1996); G. Barbarella, M. Zambianchi, A. Bongini, and L. Antolini, *J. Org. Chem.*, **61**, 4708 (1996); E. H. Elandaloussi, P. Frere, P. Richomme, J. Orduna, J. Garin, and J. Roncali, *J. Am. Chem. Soc.*, **119**, 10774 (1997); Ll. Fajari, E. Brillas, C. Aleman, and L. Julia, *J. Org. Chem.*, **63**, 5324 (1998); J. C. Horne and G. J. Blanchard, *J. Am. Chem. Soc.*, **120**, 6336 (1998); A. K. Mohanakrishnan, M. V. Lakshmikantham, C. McDougal, M. P. Cava, J. W. Baldwin, and R. M. Metzger, *J. Org. Chem.*, **63**, 3105 (1998); I. Jestin, P. Frere, N. Mercier, E. Levillain, D. Stievenard, and J. Roncali, *J. Am. Chem. Soc.*, **120**, 8150 (1998); S. Huang and J. M. Tour, *J. Org. Chem.*, **64**, 8898 (1999); E. M. Breitung, C.-F. Shu, and R. J. McMahon, *J. Am. Chem. Soc.*, **122**, 1154 (2000) and many other references cited therein.

2 H. Higuchi, N. Hayashi, H. Koyama, and J. Ojima, *Chem. Lett.*, **1995**, 1115; H. Higuchi, T. Nakayama, H. Koyama, J. Ojima, T. Wada, and H. Sasabe, *Bull. Chem. Soc. Jpn.*, **68**, 2363 (1995).

3 a) H. Higuchi, S. Yoshida, Y. Uraki, and J. Ojima, *Bull. Chem. Soc. Jpn.*, **71**, 2229 (1998). b) H. Higuchi, H. Koyama, N. Hayashi, and J. Ojima, *Tetrahedron Lett.*, **37**, 1617 (1996); H. Higuchi, H. Koyama, N. Hayashi, J. Ojima, T. Wada, and H. Sasabe, *Mol. Cryst. Liq. Cryst. Sci. Technol.*, **B15**, 209 (1996); V. Hernandez, S. C. Losada, J. Casado, H. Higuchi, and J. T. L. Navarrete, *J. Phys. Chem.*, **104**, 661(2000).

4 T. Wada, L. Wang, D. Fichou, H. Higuchi, J. Ojima, and H. Sasabe, *Mol. Cryst. Liq. Cryst. Sci. Technol.*, **B255**, 149 (1994); H. Higuchi, Y. Uraki, H. Yokota, H. Koyama, J. Ojima, T. Wada, and H. Sasabe, *Bull. Chem. Soc. Jpn.*, **71**, 483 (1998).

5 R. W. Wagner, T. E. Johnson, and J. S. Lindsey, *J. Am. Chem. Soc.*, **118**, 11166 (1996); J.-S. Hsiao, B. P. Krueger, R. W. Wagner, T. E. Johnson, J. K. Delaney, D. C. Mauzerall, G. R. Fleming, J. S. Lindsey, D. F. Bocian, and R. J. Donohoe, *J. Am. Chem. Soc.*, **118**, 11181 (1996); J. Seth, V. Palaniappan, R. W. Wagner, T. E. Johnson, J. S. Lindsey, and D. F. Bocian, *J. Am. Chem. Soc.*, **118**, 11194 (1996); J.-P. Strachan, S. Gentemann, J. Seth, W. A. Kalsbeck, J. S. Lindsey, D. Holten, and D. Bocian, *J. Am. Chem. Soc.*, **119**, 11191 (1997); H. Levanon, T. Galili, A. Regev, G. P. Wiederrecht, W. A. Svec, and M. R. Wasielewski, *J. Am. Chem. Soc.*, **120**, 6366 (1998); M. Graca, H. Vicente, L. Jaquinod, and K. M. Smith, *Chem. Commun.*, **1999**, 1771; H. L. Anderson, *Chem. Commun.*, **1999**, 2323; J. J. Piet, P. N. Taylor, H. L. Anderson, A. Osuka, and J. M. Warman, *J. Am. Chem. Soc.*, **122**, 1749 (2000); H. Tsue, H. Imahori, T. Kaneda, Y. Tanaka, T. Okada, K. Tamaki, and Y. Sakata, *J. Am. Chem. Soc.*, **122**, 2279 (2000) and many other references cited therein.

6 H. Higuchi, H. Yamamoto, J. Ojima, and G. Yamamoto, *J. Chem. Soc., Perkin Trans. 1*, **1993**, 975; H. Higuchi, H. Yamamoto, J. Ojima, and G. Yamamoto, *Bull. Chem. Soc. Jpn.*, **66**, 2323 (1993).

7 H. Imahori, H. Higuchi, Y. Matsuda, A. Itagaki, Y. Sakai, J. Ojima, and Y. Sakata, *Bull. Chem. Soc. Jpn.*, **67**, 2500 (1994).

8 H. Higuchi, H. Nishi, J. Ojima, T. Wada, and H. Sasabe, *Nonlinear Optics*, **22**, 337 (1999).

9 A part of this work on the OEP–DHBT–OEP system was preliminarily reported; H. Higuchi, T. Ishikura, K. Miyabayashi, M. Miyake, and K. Yamamoto, *Tetrahedron Lett.*, **40**, 9091 (1999).

10 D. P. Arnold, A. W. Johnson, and M. Mahendran, *J. Chem. Soc., Perkin Trans. 1*, **1978**, 366.

11 K. Sonogashira, Y. Tohda, and N. Hagihara, *Tetrahedron Lett.*, **16**, 4467 (1975).

12 G. Eglinton and A. R. Galbraith, *Chem. Ind.*, **1956**, 737.

13 R. M. Kellogg, A. P. Schaap, E. T. Harper, and H. Wynberg, *J. Org. Chem.*, **33**, 2902 (1968); R. M. Kellogg, A. P. Schaap, and H. Wynberg, *J. Org. Chem.*, **34**, 343 (1969).

14 a) H. Mao, B. Xu, and S. Holdcroft, *Macromolecules*, **26**, 1163 (1993). b) M. D'Auria and G. Mauriello, *Tetrahedron Lett.*, **36**, 4883 (1995).

15 K. E. Milgram, F. M. White, K. L. Goodner, C. H. Watson, D. W. Koppenaal, C. J. Barinaga, B. H. Smith, J. D. Winefordner, A. G. Marshall, R. S. Houk, and J. R. Eyler, *Anal. Chem.*, **69**, 3714 (1997); A. G. Marshall, C. L. Hendrickson, and G. S. Jackson, *Mass Spectrom. Rev.*, **17**, 1 (1998); K. Miyabayashi, K. Suzuki, T. Teranishi, Y. Naito, K. Tsujimoto, and M. Miyake, *Chem. Lett.*, **2000**, 172.

16 a) T. R. Janson and J. J. Katz, in "The Porphyrins," ed by D. Dolphin, Academic Press, New York (1978), Vol. IV, pp. 1–59. b) R. Ziessel, *Synthesis-Stuttgart*, **1999**, 1839; R. Purrelo, S. Gurrieri, and R. Lauceri, *Coord. Chem. Rev.*, **192**, 683 (1999); H. L. Anderson, *Chem. Commun.*, **1999**, 2323; A. K. Burrell, B. M. Jones, S. B. Hall, D. L. Officer, D. C. W. Reid, and K. Y. Wild, *J. Inclusion Phenom. Macrocycl. Chem.*, **35**, 185 (1999) and many other references cited therein.

17 E. D. Becker and R. B. Bradley, *J. Chem. Phys.*, **31**, 1413 (1959); R. J. Abraham, *Mol. Phys.*, **4**, 145 (1961).

18 H. Fischer and W. Neumann, *Justus Liebigs Ann. Chem.*, **494**, 225 (1932); J. W. Buchler, in "The Porphyrins," ed by D. Dolphin, Academic Press, New York (1978), Vol. I, pp. 389–483.

19 Further studies on self-association of the OEP–DHBT–OEP system are now in progress from the viwpoints of concentration-, temperature-, and solvent-effects. The results will be reported elsewhere in detail.

20 R. J. Abraham, G. R. Bedford, D. McNeillie, and B. Wright, *Org. Magn. Reson.*, **14**, 418 (1980).

21 H. L. Anderson, *Inorg. Chem.*, **33**, 972 (1994).

22 H. Higuchi, M. Takeuchi, and J. Ojima, *Chem. Lett.*, **1996**, 593; H. Higuchi, M. Shinbo, M. Usuki, M. Takeuchi, Y. Hasegawa, K. Tani, and J. Ojima, *Bull. Chem. Soc. Jpn.*, **72**, 1887 (1999); H. Higuchi, M. Shinbo, M. Usuki, M. Takeuchi, K. Tani, and K. Yamamoto, *Bull. Chem. Soc. Jpn.*, **73**, 1259 (2000).

23 W. T. Simpson, *J. Chem. Phys.*, **17**, 1218 (1949); J. W. Buchler and L. Puppe, *Liebigs Ann. Chem.*, **740**, 142 (1970); M. Gouterman, in "The Porphyrins," ed by D. Dolphin, Academic Press, New York (1978), Vol. III, pp. 1–165.

24 H. Imahori, Y. Tanaka, T. Okada, and Y. Sakata, *Chem. Lett.*, **1993**, 1215.

25 D. P. Arnold and L. J. Nitschinsk, *Tetrahedron*, **46**, 8781 (1992).

26 C. X. Cui, M. Kertesz, *Phys. Rev.*, **B40**, 966 (1989); R. M. S. Maior, K. Hinkelmann, H. Eckert, and F. Wudl, *Macromole-*

cules, **23**, 1268 (1990).

27 R. Takigawa, Y. Kai, G. V. Ponomarev, K. Sugiura, V. V. Borovkov, T. Kaneda, and Y. Sakata, *Chem. Lett.*, **1993**, 1071.

28 T. Sugiyama, T. Wada, and H. Sasabe, *Synth. Met.*, **28**, 323 (1989); H. Okawa, T. Hattori, A. Yanase, Y. Kobayashi, A. Carter, M. Sekiya, A. Kaneko, T. Wada, A. Yamada, and H. Sasabe, *Mol. Cryst. Liq. Cryst. Sci. Technol.*, **B3**, 169 (1992).

29 Syntheses of the diacetylene-group connected OEP–(HH DHBT) and OEP–(TT DHBT) derivatives and the related ones with **17** and **18** are under way. Their electronic and electrochemical properties will be reported in detail elsewhere.

30 J.-H. Fuhrhop, K. M. Kadish, and D. G. Davis, *J. Am. Chem. Soc.*, **95**, 5140 (1973).

31 H. H. Inhoffen, J.-H. Fuhrhop, H. Voigt, and H. Brockmann, Jr., *Justus Liebigs Ann. Chem.*, **695**, 133 (1966).

32 D. Arnold, A. W. Johnson, and M. Winter, *J. Chem. Soc., Perkin Trans. 1*, **1977**, 1643.